Journal for ImmunoTherapy of Cancer

Combination of radiotherapy and suppression of Tregs enhances abscopal antitumor effect and inhibits metastasis in rectal cancer

Dengbo Ji,[1] Can Song,[2,3] Yongheng Li,[4] Jinhong Xia,[1] Yanjing Wu,[5] Jinying Jia,[1] Xinxin Cui,[1] Songmao Yu,[4] Jin Gu [1,3,6]

To cite: Ji D, Song C, Li Y, *et al*. Combination of radiotherapy and suppression of Tregs enhances abscopal antitumor effect and inhibits metastasis in rectal cancer. *Journal for ImmunoTherapy of Cancer* 2020;**8**:e000826. doi:10.1136/jitc-2020-000826

► Additional material is published online only. To view, please visit the journal online (http://dx.doi.org/10.1136/jitc-2020-000826).

DJ, CS, YL, JX and YW contributed equally.

Accepted 27 September 2020

Check for updates

© Author(s) (or their employer(s)) 2020. Re-use permitted under CC BY-NC. No commercial re-use. See rights and permissions. Published by BMJ.

For numbered affiliations see end of article.

Correspondence to
Dr Jin Gu; zlguj@bjmu.edu.cn

ABSTRACT

Background Distant metastasis is the major cause of mortality in patients with locally advanced rectal cancer (LARC) following neoadjuvant chemoradiotherapy. Local radiotherapy can trigger an abscopal response to metastatic tumor cells. However, the abscopal effect is a rare event. CD4+ regulatory T (Treg) cell is a highly immune-suppressive subset which impedes immune surveillance against cancer, prevents the development of effective antitumor immunity and promotes tumor progression. We assume that the exploitation of the proimmunogenic effects of radiotherapy with anti-CD25 or anti-Cytotoxic T-Lymphocyte Associated Protein 4 (anti-CTLA4) monoclonal antibodies (mAbs) may enhance the local and abscopal effects in rectal cancer and improve the therapeutic outcome.

Methods mRNA expression profiling of 81 pretreatment biopsy samples from LARC patients who received neoadjuvant radiotherapy (nRT) was performed to analyze the correlation between gene expression and prognosis. A retrospective analysis of patients with rectal cancer with distant metastasis or synchronous extracolonic cancers was performed to evaluate the abscopal effect of radiotherapy on rectal cancer. Two different dual-tumor mouse models were established to investigate the efficacy of single dose and dose-fractionated radiotherapy combined with anti-CD25 or anti-CTLA4 and anti-Programmed cell death 1 ligand 1 (anti-PD1) mAbs on the local tumor growth and liver metastasis. The univariate Cox regression analysis, one-way analysis of variance, Dunnett's test, a mixed-effect linear model and Kaplan-Meier survival analysis were used to calculate p values.

Results The proportion of Tregs in pre-nRT biopsies was negatively correlated with prognosis (p=0.007). The retrospective analysis showed that regressing liver metastases were infiltrated by CD8+ T cells. In contrast, stable/progressing metastases and synchronous extracolonic cancers were characterized by PD1+ T cells and Tregs infiltration. Animal experiment results demonstrated that the combination of radiotherapy and anti-CD25/CTLA4 mAb resulted in a significant increase in CD8+ T cells and CD8+/CD4+ ratio in primary and secondary tumors compared with the irradiation alone group (all p<0.05 or p<0.01). The combined treatment was able to decrease Tregs, PD1+CD8+ and PD1+CD4+ T cells (p<0.05), suppress locally irradiated and distal unirradiated tumor growth, and improve overall survival rate. Radiotherapy in conjunction with anti-CTLA4 reduced liver metastasis (p<0.05).

Conclusions These data indicated that radiotherapy plus depletion of Tregs was able to improve the antitumor response and generate an abscopal effect.

BACKGROUND

Colorectal cancer (CRC) is one of the most common types of carcinoma throughout the world. Neoadjuvant chemoradiotherapy (nCRT), followed by surgery with a total mesorectal excision (TME), has become the standard treatment for locally advanced rectal cancer (LARC).[1] Although nCRT significantly improved patients' local recurrence-free survival, neither overall survival (OS) nor metastasis-free survival showed improvement.[2–4] More attention has turned to improve distant disease control and OS, leading to the search for more effective treatment strategies.

Many previous works indicate that radiotherapy could produce systemic, immune-mediated antitumor and antimetastatic effects.[5] Local radiotherapy may cause regression of metastatic cancer at distant sites that are not irradiated. This effect is called the abscopal effect. The abscopal effect has been reported for several cancers, including melanoma,[6] renal cell carcinoma,[7] breast cancer,[8] hepatocellular carcinoma[9] and other metastatic solid tumors.[10] There are only 46 cases of the clinical abscopal effects from radiotherapy reported between 1969 and 2014.[11] Radiotherapy can enhance antitumor immunity, but can also induce immunosuppressive responses which result in antitumor CD8+ T cells primed by radiotherapy being unable to overcome the suppressive effect in the tumor microenvironment.[12]

J Immunother Cancer: first published as 10.1136/jitc-2020-000826 on 26 October 2020. Downloaded from http://jitc.bmj.com/ on April 28, 2024 by guest. Protected by copyright.

The discovery that combining radiotherapy with checkpoint blockade may enhance the abscopal effect has generated great interest.[13] Many preclinical studies have investigated different combination regimens in various types of cancer. Radiation and dual checkpoint blockade by anti-CTLA-4 and anti-Programmed cell death 1 ligand 1 (anti-PD-L1) or anti-PD-1 improved responses and long-term survival of mice with melanoma due to anti-CTLA-4-mediated depletion of intratumoral regulatory T (Treg) cells, and reinvigoration of exhausted T cells by anti-PD-L1.[13] The combination of an agonist αCD40 antibody, RT and dual immune checkpoint blockade (ICB) with αCTLA-4 and αPD-1 eradicated irradiated and unirradiated pancreatic ductal adenocarcinoma, generating long-term immunity.[14] Abscopal responses were reported in mice bearing breast, melanoma and colorectal bilateral tumors following local radiation to one tumor combined with an agonistic anti-CD137 (4-1BB) and a neutralizing PD-1 antibody.[15]

Here, we analyzed prognosis associated gene expression by mRNA expression profiling of pre-neoadjuvant radiotherapy (nRT) biopsies and their enriched pathway. Measurement of serum cytokine/chemokine level and analysis of tumor infiltrating lymphocytes (TILs) were performed to investigate the influence of the tumor environment on the outcome of rectal cancer patients treated with nCRT. A retrospective analysis of patients with rectal cancer with distant metastasis or synchronous extracolonic cancers was performed to evaluate the abscopal effect of radiotherapy on rectal cancer. We investigated the efficacy of radiotherapy in combination with transient Treg depletion transiently using anti-CD25 on local and distant tumor responses as well as animal survival. We further investigated the efficacy of radiotherapy combined with anti-CTLA4 and PD1 on inhibiting and preventing liver metastasis.

METHODS AND MATERIALS

Patients and samples

All patients were informed prior to the study and a consent form was signed by each participant.

Cohort 1 was composed of biopsy samples from 81 LARC patients before nRT and resection. All the samples were from patients who received nRT and surgical resections between 2004 and 2010 at the Peking University Cancer Hospital and Institute (Beijing, China). Inclusion criteria were: (1) pathological confirmation of rectal adenocarcinoma; (2) tumor staged as T3–4 or any T, n+ by endorectal ultrasonography, pelvic MRI or CT; (3) no evidence of distant metastasis. Patients with the following characteristics were excluded: (1) previous chemotherapy or pelvic radiation; (2) presence of any other malignant disorders or other chronic diseases. All patients were treated with intermediate-fraction nRT (30 Gy/10 fractions), followed by a TME surgery. The samples were used for microarray analyzes. Biopsies were collected by proctoscopy and stored immediately in RNAlater (Qiagen) and then stored at −80°C until use.

Cohort 2 consisted of 90 LARC patients who received nCRT and surgical resections between 2014 and 2016. Inclusion criteria were: (1) pathological confirmation of rectal adenocarcinoma; (2) tumor staged as T3–4 or any T, n+ by endorectal ultrasonography, pelvic MRI or CT; (3) no evidence of distant metastasis. Patients with the following characteristics were excluded: (1) previous chemotherapy or pelvic radiation; (2) presence of any other malignant disorders or other chronic diseases. The radiotherapy regimen consisted of a 50.6 Gy dose delivered in 22 fractions with concurrent capecitabine treatment at a dose of 825 mg/m^2 orally two times a day for 5 weeks. Blood samples from pretreatment and paired post-operation were collected and processed within 1 hour based on protocols of NCI's Early Detection Research Networks. Sera obtained were aliquoted immediately and stored at −80°C until used for cytokine/chemokine measurement.

To evaluate the abscopal effect of radiotherapy on rectal cancer, we performed a retrospective analysis of patients with rectal cancer with synchronous distant metastasis or concomitant extracolonic cancers. Inclusion criteria were: (1) diagnosis of rectal adenocarcinoma by biopsy; (2) with distant metastasis at the pretreatment or during nCRT; (3) or with concomitant extracolonic cancers; (4) underwent nCRT. Patients without clinical/pathological characteristics and lack of follow-up information were excluded. In the period of July 2004 and September 2017, there were 533 patients with rectal cancer who received nCRT. In total, 13 patients with rectal cancer were registered in cohort 3 which included 10 patients with liver or lung metastasis and 3 patients with concomitant extracolonic cancer. Among of 10 patients with synchronous distant metastasis, two patients were found to have liver metastases during nCRT by preoperation CT. All patients received nCRT and rectal cancer surgical resections and had at least one distinct measurable size of tumor mass. The radiotherapy regimen consisted of a 50.6 Gy dose delivered in 22 fractions. For patient with synchronous esophagus cancer, the concurrent chemotherapy regimens were capecitabine with taxol and nedaplatin treatment. For other patients, the concurrent chemotherapy regimens were primarily capecitabine-based, with or without oxaliplatin treatment. Pretreatment and post-treatment CT or MRI was obtained to follow tumor response and assess abscopal responses. Response evaluation by imaging was performed within 60 days of the nCRT treatment using Response Evaluation Criteria in Solid Tumor (RECIST) V.1.121. Primary tumor or distant metastasis tissues obtained from cohort 3 were used to investigate the immune infiltration status using multiplex fluorescence staining. One patient with rectal cancer (case 14) with metachronous liver metastasis was also assessed for immune infiltration status of the tumor metastasis. Case 14 received nCRT and rectal cancer surgical resection and developed liver metastasis 2 years after surgery.

J Immunother Cancer: first published as 10.1136/jitc-2020-000826 on 26 October 2020. Downloaded from http://jitc.bmj.com/ on April 28, 2024 by guest. Protected by copyright.

A summary of the clinical characteristics of these patients is shown in online supplemental table S1–S3.

Assessment of treatment response and tumor downstaging

The seventh edition of the American Joint Committee on Cancer TNM system was used for Pathological staging.[16] NRT effect was evaluated after surgery by specialized gastrointestinal pathologists using the tumor regression grade (TRG) system as follows: grade 0: complete regression, no tumor cells; grade 1: single or small groups of tumor cells, moderate response; grade 2: residual cancer outgrown by fibrosis, minimal response; grade 3: minimal or no tumor cells killed, poor response.

RNA isolation and microarray analyses

Total RNA from cohort 1 biopsy samples was isolated using TRIzol reagent (Life technologies, Carlsbad, California, USA), according to the manufacturer's instructions, and purified by using the RNeasy Mini Kit (Qiagen, Germany). RNA samples of each group were subsequently used to generate fluorescence-labeled cRNA targets for the Affymetrix Human U133 Plus 2 arrays (Affymetrix, Santa Clara, California, USA). The labeled cRNA targets were then hybridized on slides. After hybridization, slides were scanned by GeneChip Scanner 3000 (Affymetrix). Data were extracted with Command Console Software V.4.0 (Affymetrix). Raw data were normalized by the MAS V.5.0 algorithm and Gene Spring Software V.12.6.1 (Agilent technologies, Santa Clara, California, USA). The microarray experiments were performed following the protocol of Affymetrix Inc.

Serum cytokine/chemokine measurement

Blood samples were collected at baseline and 1 day after operation. Sera obtained from blood samples were used for serum cytokine/chemokine measurements. Serum was separated by centrifugation at 2000 g for 10 min at 4°C to remove the cellular components. Serum cytokine/chemokine levels were measured using the Human Cytokine/Chemokine Magnetic Bead Panel protocol from the Milliplex Map Kit (EMD Millipore, Billerica, Massachusetts, USA), following the manufacturer's instructions. The kit was used to analyzed 38 cytokines: interleukin-1 alpha (IL-1a), IL-1b, IL-1RA, IL-2, IL-3, IL-4, IL-5, IL-6, IL-7, IL-8, IL-9, IL-10, IL-13, IL-15, IL-17, IL-12P40, IL-12P70, epidermal growth factor, eotaxin, granulocyte colony-stimulating factor (G-CSF), granulocyte-macrophage CSF (GM-CSF), interferon alpha-2 (IFN), IFNγ, IFN gamma-induced protein 10, monocyte chemotactic protein-1 (MCP-1), MCP-3, MIP-1a, MIP-1b, tumor necrosis factor alpha (TNF-α), TNF-β, vascular endothelial growth factor, fibroblast growth factor 2, transforming growth factor alpha, Flt-3 ligand, fractalkine, growth regulated oncogene, macrophage-derived chemokine and soluble CD40 ligand (sCD40L). All measurements were performed on a Luminex 200 analyzer (Luminex, Austin, Texas, USA). Analysis of the cytokine/chemokine median fluorescence intensity was performed using the Milliplex Analyst (V.5.1).

Multiplex immunofluorescence staining and image analysis

Tissues consisting of primary tumor or distant metastasis were obtained from cohort 3 patients and case 14 who underwent surgical resections. All samples were collected immediately after resection and fixed in 10% formalin for paraffin embedding. The paraffin-embedded samples were used for the fluorescent multiplex immunofluorescence staining. Opal 7-Color Fluorescent immunohistochemistry (IHC) Kit (PerkinElmer, Massachusetts, USA) was used to detect the signals. The Opal protocol was followed except that slide deparaffination, antigen retrieval and antibody stripping were all performed using AR 6.0 buffers (NEL811001KT, PerkinElmer). The five-plex staining was performed in the following order: anti-CD4 (ab133616, Abcam) stained with Opal 520, anti-CD8 (ab101500, Abcam) stained with Opal 570, anti-PD1 (ab52587, Abcam) stained with Opal 690, anti-FoxP3 (ab4728, Abcam) with Opal 620. All primary antibody solutions were incubated for 30 min at room temperature. Nuclei were stained with DAPI prior to mounting in Prolong Diamond Antifade Mountant (Thermo Fisher). Stained slides were scanned and images were analyzed by Vectra Polaris multispectral slides imaging system and inForm tissue finder image analysis software (PerkinElmer).

Cell lines

The MC38 cell line was purchased from National Infrastructure of Cell Line Resource (Beijing, China) and was maintained in Roswell Park Memorial Institute (RPMI) 1640 with 10% fetal bovine serum (Gibco, Carlsbad, California, USA), penicillin sodium (100 U/mL), and streptomycin sulfate (100 mg/mL) in humidified 5% CO_2 at 37°C. The cell line was tested and authenticated by Short Tandem Repeat (STR) profiling. Cells were routinely tested for mycoplasma infection and used only when negative. Cells were passaged a maximum of 3–4 times in vitro before they were used in in vivo experiments.

In vivo mouse studies

Male C57BL/6 mice aged between 4 and 6 weeks were purchased from Beijing Vitalriver Experimental Animal Technology (Beijing, China). Mice were maintained in a pathogen-free facility and used in accordance with the institutional guidelines for animal care.

The mice were bilaterally inoculated with MC38 cells on the right leg (1×10^5 cells) and left flank (5×10^4 cells) by subcutaneous injection on day 0. For single dose radiotherapy, the right leg tumor was irradiated with 12 Gy on day 12. Anti-CD25 antibody (BioXCell) was intraperitoneally administered on days 9, 16 and 23. For dose-fractionated radiotherapy model (5 fractions of 2.3 Gy each), the right leg tumor was irradiated with 2.3 Gy on day 16, 17, 18, 19, 20. Anti-CD25 antibody (BioXCell) was intraperitoneally administered on days 14, 19 and

J Immunother Cancer: first published as 10.1136/jitc-2020-000826 on 26 October 2020. Downloaded from http://jitc.bmj.com/ on April 28, 2024 by guest. Protected by copyright.

24. All irradiation was performed using the Edge linear accelerator (Varian Medical Systems, Palo Alto, California, USA). Antibodies used for in vivo ICB experiments were given intraperitoneally at a dose of 250 µg/mouse and include: anti-CD25 (clone PC-61.5.3) and rat IgG1 isotype (clone TNP6A7) (all from BioXCell). The tumor volumes were measured using CT scans and MRI once a week. The tumor size was measured using calipers every 3 days. Volume was calculated using the formula $L \times A \times B \times 0.52$, where L is the longest dimension and A and B are long and short diameters of the largest coronal section, respectively. Differences in survival were determined for each group by the Kaplan-Meier method. The overall p value was calculated by the log-rank test. In vivo studies were terminated either when the animals succumbed to death or when tumor burden reached a protocol-specified size of 1.5 cm in maximum dimension as suggested previously.[13]

For synchronous CRC liver metastasis mouse models, mice were subcutaneously inoculated with MC38 cells on the right leg (1×10^5 cells) and under the capsular of the spleen (1×10^5 cells) on day 0. Cells were surgically injected into the spleen through an abdominal incision under anesthesia. After injection, the spleen was gently returned to abdominal cavity and homoeostasis was resumed. For single dose radiotherapy, the right leg tumor site was irradiated with 8 Gy on day 9. Blocking antibodies (anti-CTLA4, clone 9H10, anti-PD1, clone RMP1-14 and rat IgG1 isotype, clone TNP6A7, all from BioXCell) were given intraperitoneally at a dose of 250 µg/mouse on days 6, 9 and 12. For dose-fractionated radiotherapy model (5 fractions of 2.3 Gy each), the right leg tumor was irradiated with 2.3 Gy on day 13, 14, 15, 16, 17. Blocking antibodies (anti-CTLA4, anti-PD1 and rat IgG1 isotype) were intraperitoneally administered on days 10, 13 and 16. All irradiation was performed using the Edge linear accelerator (Varian Medical Systems). The tumor volumes of the right leg were measured using calipers every 3 days. Four weeks after surgery, mice were euthanized and the livers were obtained to determine the hepatic metastatic foci.

The MC38 cells with stably transfected luciferin were used to observe liver metastasis. The tumor burden on liver was quantified by in vivo bioluminescence imaging and ex vivo fluorescence imaging of whole livers using an In Vivo Imaging System (IVIS) Spectrum-CT (Perkin-Elmer). Data were analyzed using Living Image V.4.0 Software (Caliper Life Sciences).

Flow cytometric analysis

The tumor masses from mice were removed, minced and processed using a gentle MACS dissociator and a murine tumor dissociation kit (Miltenyi Biotec). The cell suspensions were filtered through 70 µm cell strainers and washed with PBS. Single-cell suspensions were counted and stained with CD45 (APC, clone 30-F11), CD3 (BUV395, clone 145–2C11), CD8 (PE, clone 53–6.7), CD4 (BUV737, clone GK1.5), CD25 (BB515, clone PC61), CD152 (APC, clone UC10-4F10-11), CD69 (PerCP-Cy5.5, clone H1.2F3), CD127 (APC, clone SB/199) and CD44 (PE, clone IM7). The intracellular staining of Granzyme B (Alexa Fluor 647, clone D2H2F) and Foxp3(PE, clone MF23) was performed using the Transcription Factor Staining Buffer Set (BD). For quantification of absolute number of cells, cell counts were normalized by tumor mass. All flow cytometric analyzes were performed using FACSAria II flow cytometer (BD Biosciences, San Jose, California, USA) and the data were processed using FlowJo software (Tree Star). Gating strategy was shown in online supplemental figure 1.

Immunohistochemical analysis

Tumor tissue was freshly taken from mice and processed for IHC. IHC was performed on formaldehyde-fixed and paraffin-embedded 3–4 µm tissue sections, using rabbit monoclonal anti-mouse PD-1 (clone EPR20665, Abcam, USA), anti-mouse CD4 (clone EPR19514, Abcam, USA), anti-mouse CD8 (clone EPR21769, Abcam, USA) and anti-mouse FOXP3(clone FJK-16s, eBioscience). All images were examined by two experienced pathologists independently. The slides were then scanned into high-resolution images using Aperio Versa 200 (Aperio, Vista, California, USA). The images were then visualized and the percent of CD4+, CD8+FOXP3+ and PD1+ cells (eg, number of positive cells/total number of cells) were quantified using the software Aperio Image Scope (Aperio).

Statistics

The univariate Cox regression analysis was performed to examine the relationship between the gene expression levels in patients and the OS from cohort 1 to determine the genes which could potentially be of functional significance in prognosis of LARC patients treated with nRT. OS was defined as the time from the date of surgery until death from any reason. Genes that were significantly related to patient survival were identified ($p<0.05$). HRs from univariate Cox regression analysis were used to identify which genes were associated with death from recurrence of cancer or any other reason. Protective genes were defined as those with HR for death <1. High-risk genes were defined as those with HR for death >1. The analyzes were performed in the R programming language (V.3.2.3).

One-way analysis of variance (ANOVA) and Dunnett's test were used to compare immune cell fraction differences between treated groups and control groups. A mixed-effect linear model was used to determine significance of differences in tumor growth. The log-rank test was used to compare Kaplan-Meier survival curves. The cut-off values of immune cell fractions and cytokine levels were selected by X-title program.[17] For abscopal analysis, DFS was defined as the time from the date of surgery until first recurrence or death due to any reasons, whichever observed first. All tests were two sided and the level of statistical significance was set at $p<0.05$. Statistical analyzes were performed using GraphPad Prism V.6.

J Immunother Cancer: first published as 10.1136/jitc-2020-000826 on 26 October 2020. Downloaded from http://jitc.bmj.com/ on April 28, 2024 by guest. Protected by copyright.

Data and materials availability

The GEO accession number is GSE119409.

RESULTS

Immune activity pre-nRT correlated with prognosis in LARC

To investigate the correlation between gene expression and prognosis of LARC with nRT, mRNA expression in pretherapy biopsies of cohort 1 was profiled. By performing univariate Cox proportional hazards regression analysis for mRNA expression data, a total of 674 mRNAs related to patient OS ($p<0.05$) were identified, including 437 protective genes (HR <1) and 237 high-risk genes (HR >1). Reactome pathway analysis showed that the protective genes were enriched in the immune activation-related pathways, including cytokine signaling in immune system, signaling by IL, downstream signaling events of B cell receptor and IL-4 and 13 signaling (online supplemental table S4).

Fractions of Tregs in pre-nRT biopsies negatively correlated with prognosis of LARC

The correlation between infiltrating immune cells and prognosis of LARC with nRT was further assessed using CIBERSORT. The patients with no distant metastasis or death observed at 5 years were identified as the good prognosis group, while the patients with distant metastasis or death observed in 5 years were identified as the poor prognosis group. The results showed that the fractions of Tregs (2.9% vs 1.3%), gamma delta T cells (3.7% vs 0%) and resting CD4+ memory T cells (11% vs 5.4%) in the patients with poor prognosis were higher than that in patients with good prognosis. In the good prognosis group, the fraction of activated dendritic cells (DCs) (5.47% vs 3.18%) and macrophage M0 (11.7% vs 6.8%) were higher than that in the poor prognosis group (online supplemental figure 2A). Kaplan-Meier survival analysis showed that fractions of Tregs and resting DCs in pre-nCRT biopsies negatively correlated with disease-free survival ($p=0.007$, $p=0.001$, respectively) (online supplemental figure 2B,C). The fractions of Tregs and resting DCs were also significantly associated with poor OS ($p=0.017$, $p=0.019$, respectively) (online supplemental figure 2D,E).

Several cytokines in pre-nCRT and post-nCRT serum correlated with prognosis

To investigate the effect of serum cytokines in prognosis of LARC treated by nCRT, the level of cytokines in pre-nCRT and post-nCRT serum from cohort 2 were assayed. Kaplan-Meier analysis showed that patients with high GM-CSF (≥2.08 pg/mL), IL-2 (≥1.05 pg/mL), IL-3 (>0.49 pg/mL) or IL-4 (>3.39 pg/mL) level in pre-nCRT had a poor OS ($p=0.026$, $p=0.005$, $p=0.002$ and $p=0.007$, respectively (online supplemental figure 3A–D). While serum TNFα level post-nCRT was positively correlated with prognosis ($p=0.033$, online supplemental figure 3E).

Abscopal effect of RT on patients with rectal cancer with distant metastasis or synchronous extracolonic cancers

To investigate the abscopal efficacy of RT on patients with rectal cancer, the clinical and pathological data of rectal cancer patients with distant metastasis or synchronous extracolonic cancers which were treated with nCRT were retrospectively collected. Form July 2004 to September 2017, 533 patients with rectal cancer underwent nCRT. In all, a total of 13 patients with rectal cancer were included in cohort 3, 10 patients with liver or lung metastasis, 3 patients with synchronous extracolonic cancer (esophagus, prostatic and liver cancer). All patients received radiotherapy to the primary rectal cancer lesion. Evaluation of the unirradiated lesions by MRI or CT imaging using RECIST demonstrated that 67% (6/9) of patients with liver metastasis had a partial response (PR) as best response, 11% (1/9) had stable disease (SD), 22% (2/9) had progressive disease, these two patients had new lesions. The one patient with lung metastasis had SD, and 100%[3] of patients with synchronous extracolonic cancer had SD. All of the 13 patients evaluated by TRG had PR or complete response (CR) in the irradiated lesion. The median progression-free survival (PFS) was 14, and the median OS was not reached (figure 1A–E).

Heterogeneous immune cell infiltration in growing and regressing metastasis and synchronous extracolonic lesions

To investigate the immune infiltration status of the tumor metastasis, we used multiplex fluorescence staining to analyze the immune components of tumors. T cell markers CD4, CD8, T regulatory cell markers Foxp3 and PD-1 were detected by fluorescence costaining. In liver metastasis with a major clinical response (case 6, PR, −78%), we observed a strong CD8 +infiltrate and low Foxp3+ and PD1+ infiltration. The infiltration of CD8+PD1+, CD4+PD1+ and Foxp3+ cells increased in liver metastasis of SD patients (case 4, SD, −21%). Liver metastasis in PD patients (case 8, PD, +21%) showed higher Foxp3 positive and PD-1+CD4+ T cell infiltration, especially in the stroma. We also analyzed a metachronous liver metastasis from a rectal cancer patient with nCRT (case 14). Higher Foxp3 positive T cell infiltration was observed and these changes were pronounced in the stroma. In liver metastasis with SD and PD, we observed large numbers of infiltrating lymphocytes including CD4 and CD8 T cells at the tumor margin much more than infiltrating the tumor. In synchronous esophagus cancer (case 11, SD, −0.27%), PD-1 positive cells increased. IF analysis indicated that the increased Tregs and PD1+ T cells and the decreased effector: Treg ratios in metastatic or synchronous extracolonic cancer might be correlated with poor abscopal effect (figure 1F–G, online supplemental figure 4).

RT combined with anti–CD25 enhances control of irradiated and abscopal tumors

We first determined the expression of CD25 on TILs and found that the percentage of CD25-expressing Teff cells (CD8+=0.4%–1.6%, CD4+ FoxP3-=10.3%–19.2%)

J Immunother Cancer: first published as 10.1136/jitc-2020-000826 on 26 October 2020. Downloaded from http://jitc.bmj.com/ on April 28, 2024 by guest. Protected by copyright.

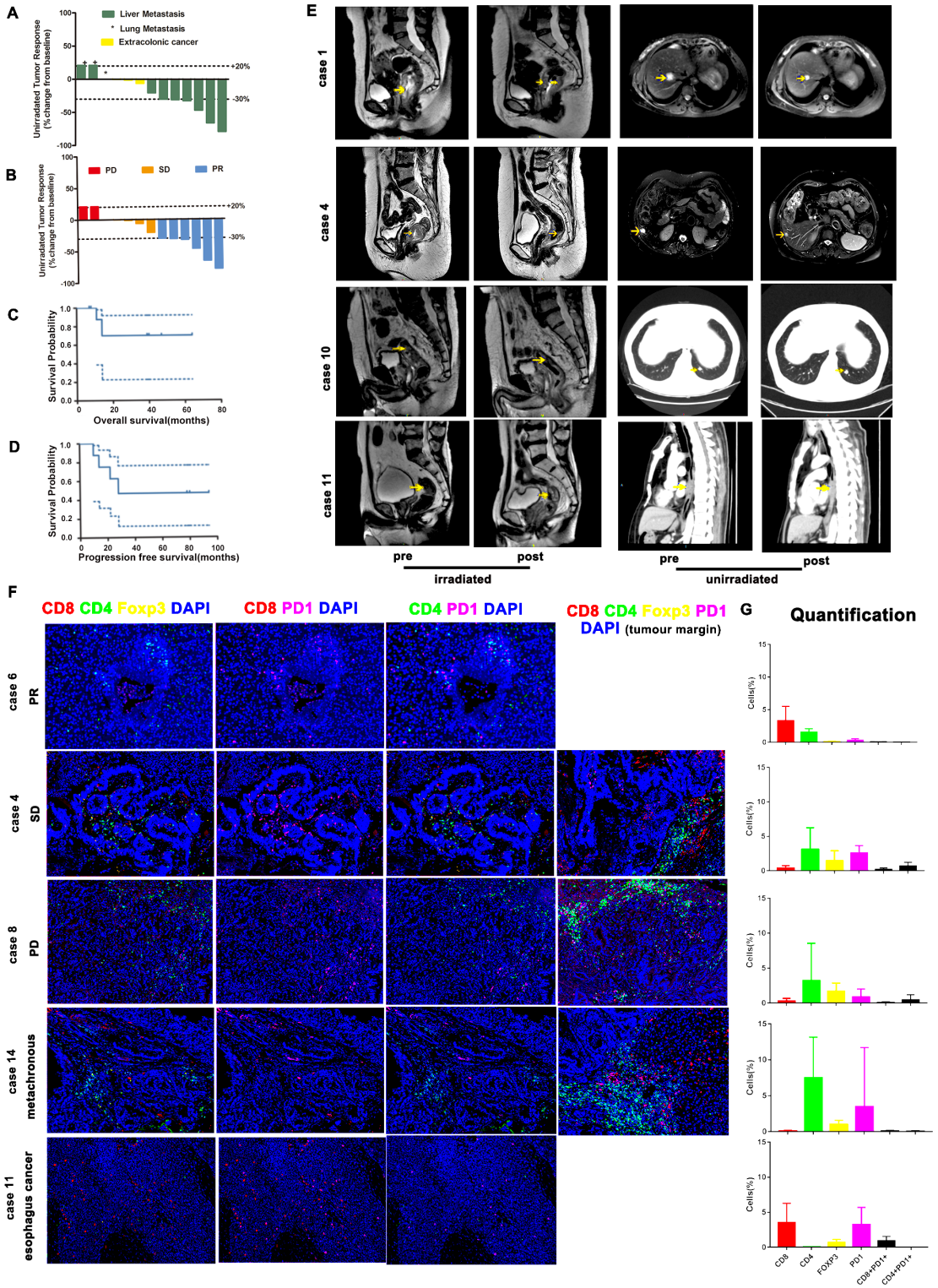

Figure 1 Abscopal effect of RT correlates with tumor infiltrating immune cells. (A) Waterfall plot of the RECIST per cent change from baseline of unirradiated tumors as measured by MRI or CT. Dashed lines are thresholds for PD (upper) and PR (lower). RECIST criteria do not include irradiated tumors. legend shows color-codes for the organs of the unirradiated tumors. *Patient with 0% change. Two patients were assigned a value of +21% for new lesions (+). (B) Legend shows color-codes for response after RT by MRI or CT (parenthesis). (C) PFS for all patients (dashed lines: 95% CI). (D) OS for all patients (dashed lines: 95% CI). (E) MRI of irradiated and unirradiated (arrows) tumors from patient case 1 (liver, PR, −66%), case 4 (liver, SD, −21%), case 10 (lung, SD, 0%) and case 11 (synchronous esophagus cancer, SD, −0.27%). (F) Representative images of immunofluorescence staining for DAPI, cytotoxic T cells (CD8+), CD4+ T cells, Tregs (CD4+FOXP3+) and immune-checkpoint PD1+ cells of case 6 (PR, −78%), case 4 (SD, −21%), 8 (PD, +21%), case 14 (metachronous liver metastasis) and case 11 (synchronous esophagus cancer, SD, −0.27%). (G) Image-based cell quantification of whole slides. OS, overall survival; PFS, progression-free survival; PR, partial response; RECIST, Response Evaluation Criteria in Solid Tumor; RT, radiotherapy; Tregs, regulatory T.

J Immunother Cancer: first published as 10.1136/jitc-2020-000826 on 26 October 2020. Downloaded from http://jitc.bmj.com/ on April 28, 2024 by guest. Protected by copyright.

was significantly lower than on Treg cells (59.2%–68.5%) (online supplemental figure 5A). To determine the optimal dose of anti-CD25, we investigated the effect of the in vivo administration of anti-CD25 mAb on a CD4+Foxp3+population in spleens and tumor tissues. As shown in online supplemental figure 5, CD4+Foxp3+ cells accounted for about 12% and 35% of CD4+ cells in spleen and tumor, respectively. In spleen, CD4+Foxp3+ cells were reduced to the maximum extent at 2–4 days after a single dose of 0.25 mg anti-CD25 mAb in vivo, and recovered completely on the fifth day. In the tumor, after a single dose of 0.25 mg anti-CD25 mAb, the CD4+Foxp3+ cells decreased to the maximum extent on days 2–4, and recovered completely on day 8. In the dose range of 0.125–0.5 mg, the spleen and tumor decreased by 37%–52% and 49%–73%, respectively. For subsequent analyzes, we used a single injection of 0.25 mg anti-CD25.

Mice bearing bilateral tumors derived from subcutaneous engraftment of MC38 colorectal carcinoma cells were used as a model to investigate the local and abscopal effects of radiotherapy in combination with anti-CD25 mAb. Mice received IgG (control), irradiation (RT+IgG), anti–CD25 or both treatments (RT+anti-CD25). For single-dose radiotherapy, radiotherapy at dose of 12 Gy was applied only to the right leg tumor site, while the left flank tumor was set outside the irradiated field. The left flank tumors were inoculated the same day with twofold fewer tumor cells. We found that RT+IgG, anti-CD25 and RT+anti-CD25 could control both local and unirradiated tumors (all p<0.0001). The best response in unirradiated tumors occurred with RT+anti-CD25. However, compared with RT, RT+anti-CD25 did not show better effect on local tumor control (figure 2A–D).

Kaplan-Meier analysis showed that RT, anti-CD25, and RT+ anti-CD25 improved the survival of mice (p=0.001). The largest improvement in survival was observed in the RT+ anti-CD25 group. When compared with RT or anti-CD25 alone, RT combined with anti-CD25 still improved the survival significantly (p=0.043, p=0.020, respectively) (figure 2E).

To mimic the regimen used in routine clinical practice, we performed dose-fractionated radiotherapy regimen (5 fractions of 2.3 Gy each). Our results showed that dose-fractionated RT+ anti-CD25 could control both local and unirradiated tumors (p=0.046, p=0.0039, respectively) (online supplemental figure 6A–C).

RT combined with anti-CD25 changes the immune tumor microenvironment in irradiated and unirradiated lesions

Antitumor immune responses depend on the proportions and functions of the cells in the tumor microenvironment. For the single-dose radiotherapy model, we compared percentages of TILs obtained on day 32 from the irradiated and unirradiated tumors in the treatment groups by flow cytometric analysis and IHC. In the irradiated tumors, combination therapy induced the increase in the percentage of CD8+ T cells and the ratio of CD8+/CD4+ relative to tumors in the control, RT or anti-CD25 alone groups (p=0.0017, p<0.0001, respectively). No significant difference was observed in the percentages of CD4+ T cells among groups. We observed that Tregs were clearly increased in RT groups compared with control. Combination therapy could significantly decrease the proportion of Tregs induced by RT (p=0.0152 for ANOVA comparing the effect across all group; p=0.0134 for RT vs IgG control; p=0.032 for RT vs combination treatment) (figure 3).

Given that the T cell surface receptor PD-1 plays a critical role in inhibiting T cell responses, we further investigated whether combination therapy might affect the expression of PD-1 and effector functions of CD8+ and CD4+ T cells in tumors. To address this question, we analyzed the expression of PD-1 on CD8+ and CD4+ T cells derived from irradiated tumors. We found that RT significantly increased the expression of PD-1 on CD8+ and CD4+ T cells. In contrast, combination of RT and anti-CD25 reversed the increase in PD-1 expression on CD8+ and CD4+ T cells conferred by RT in irradiated tumors (p=0.0021 and p=0.0009, respectively, for ANOVA comparing the effect across all group; For CD8+PD1+ T cells, p=0.0002 and p=0.0034; For CD4+PD1+ T cells, p=0.0021 and p<0.0001, the relevant comparisons are RT vs IgG and RT vs anti-CD25) (figure 3). To assess T-cell activation, we examined the expression of CD44. No significant difference was observed in the percentages of CD44+CD4+ and CD44+CD8+ T cells among the groups (online supplemental figure 7A–C). To further investigate the extent of T-cell infiltration in tumors, we analyzed the total numbers of CD8+, CD4+ T cells, Tregs, PD1+CD8 and PD1+CD4+ T cells in tumors. Our results showed that RT slightly induced CD8+ and CD4+ T cells infiltration. Combination of RT and anti-CD25 induced a significant CD8+ T cells infiltration (p=0.023). RT induced a significant increase in PD1+CD8+(p=0.0072) and PD1+CD4+ T cells (p=0.0146) numbers which could be reduced by combination therapy or anti-CD25 treatment alone (p=0.012 for PD1+CD4+ in anti-CD25 vs IgG+RT; p=0.24 for PD1+CD8+ in anti-CD25+RT vs IgG +RT). Anti-CD25 treatment could reverse the increase in Tregs induced by RT (p=0.0204) (figure 3K–P).

In the unirradiated tumors, RT, anti-CD25 or RT+ anti-CD25 increased the number of CD4+ T (p=0.003, p=0.0091 and p=0.01039, respectively). Compared with the control group, the number of CD8+ T cells in the anti-CD25 alone or combined treatment group was significantly increased (p=0.029, p=0.049, respectively), but there was no difference between the two groups. PD-1 expression significantly decreased after combination therapy as compared with control and RT alone groups (p=0.0317). Compared with the control group, the number of Foxp3 +cells in the anti-CD25 group was significantly decreased (p=0.0378). The number of Foxp3+ cells decreased in anti-CD25 alone or combination therapy group as compared with RT group, though there was no significant (p=0.0764 and p=0.3572, respectively) (figure 4).

J Immunother Cancer: first published as 10.1136/jitc-2020-000826 on 26 October 2020. Downloaded from http://jitc.bmj.com/ on April 28, 2024 by guest. Protected by copyright.

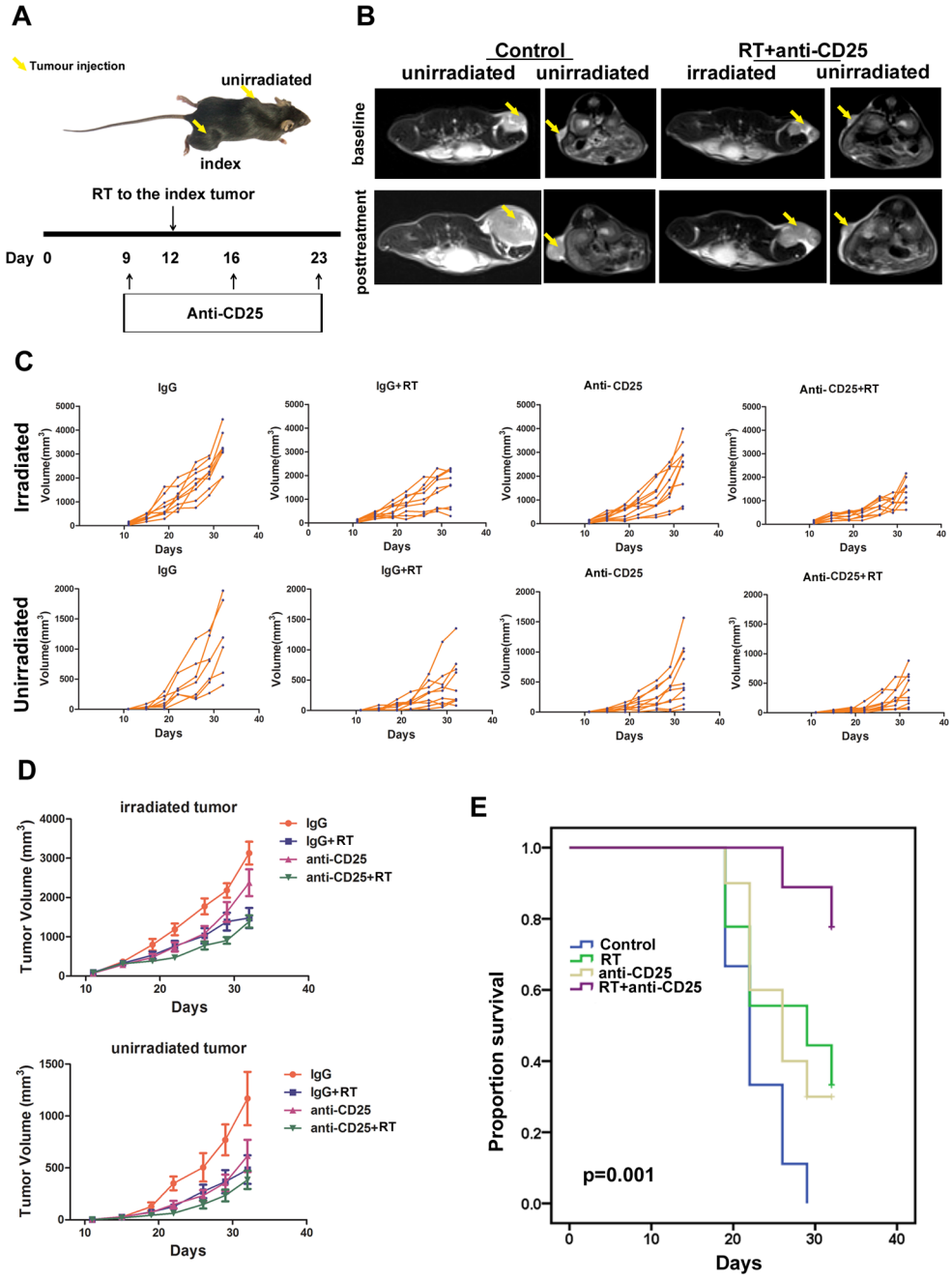

Figure 2 Single-dose RT combined with anti-CD25 enhances tumor growth control in a bilateral mouse model. (A) Schematic of the experimental setup. yellow arrow: location of transplantation. Timeline starts from original tumor implantation (day 0). Black arrows: treatments given. (B) MRI images of RT combined with anti-CD25-treated tumors and baseline/control tumors. (C, D) Total irradiated and unirradiated tumor growth for MC38 tumors after the indicated treatment. Control: IgG (n=8); RT: IgG+RT (n=8); anti-CD25 (n=8); RT combined with anti-CD25 (n=8). Using a mixed-effect linear model to compare tumor growth differences between treated groups and control groups. (E) Survival after RT and/or anti-CD25. control is an isotype-matched antibody. Using the log-rank test, statistical significance was set at p<0.05. RT, radiotherapy.

In blood, anti-CD25 significantly decreased the proportion of Tregs relative to the IgG control(p=0.0028). Combination therapy decreased the proportion of Tregs and increased the ratio of CD8+/Tregs compared with control (p=0.0108, p=0.0355, respectively). No significant difference was observed in the percentages of CD4+ and CD8+ T cells among groups. Anti-CD25 and combined therapy increased PD-1 expression in CD4+cells (p=0.039, p=0.029) (online supplemental figure 7D–I).

We also compared percentages of TILs from the irradiated and unirradiated tumors in dose-fractionated radiotherapy model. In the irradiated tumors, combination therapy induced a significant increase in the percentage of CD8+ T cells relative to tumors in the control (p=0.0233). Combination therapy did not affect the

J Immunother Cancer: first published as 10.1136/jitc-2020-000826 on 26 October 2020. Downloaded from http://jitc.bmj.com/ on April 28, 2024 by guest. Protected by copyright.

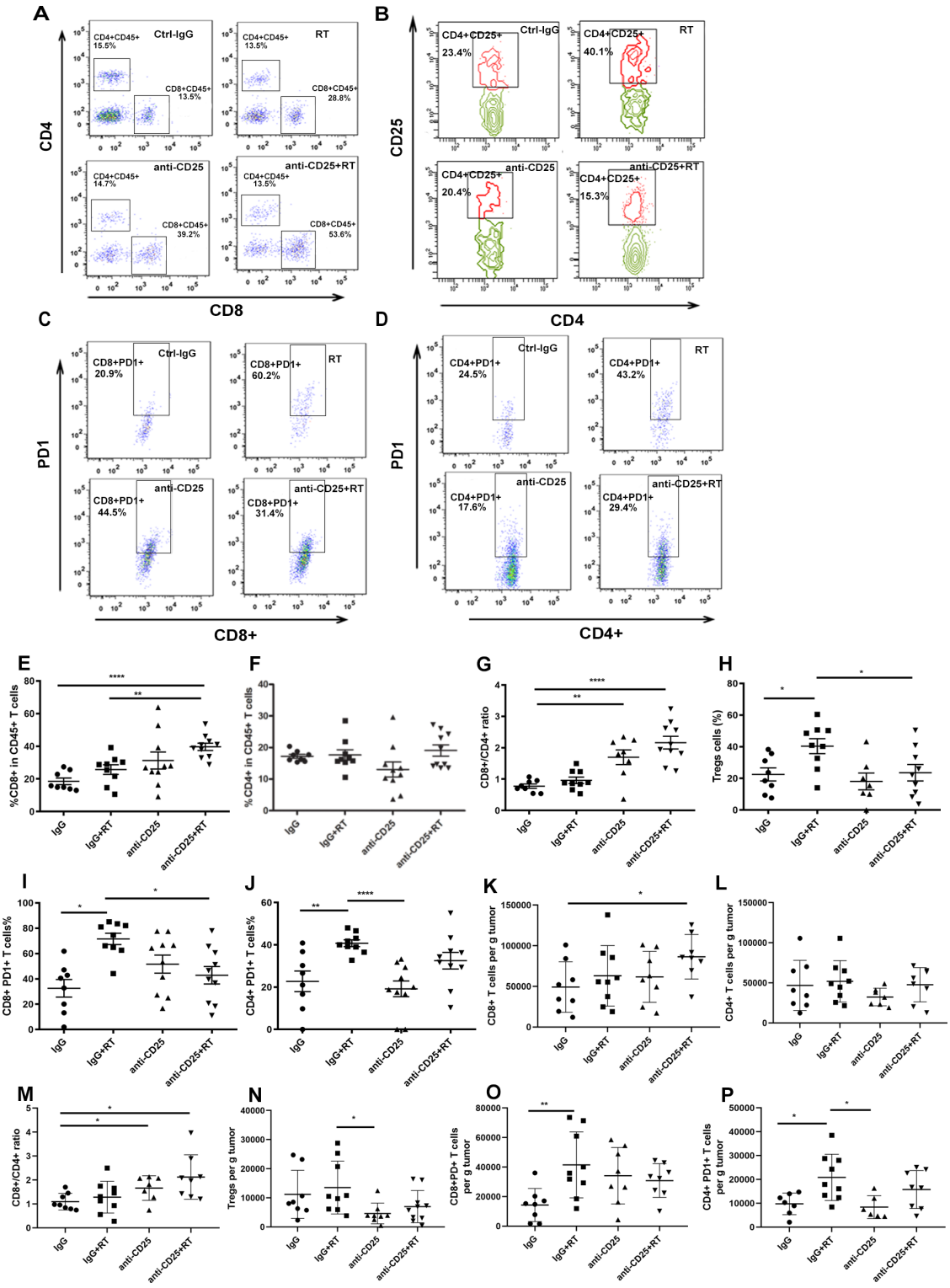

Figure 3 Single-dose RT combined with anti-CD25 changes the fractions of CD4+, CD8+, Tregs cells, PD1+CD4+ and PD1+CD8+ T cells in irradiated tumors. (A) Representative dot plots show the percentages of CD4+ and CD8+ T cells after gating on CD45+ cells analyzed by flow cytometry in the irradiated tumor-derived cell suspensions corresponding to RT, RT+ anti-CD25, anti-CD25 as indicated. (B) Representative contour plots of CD4+CD25+ T (Tregs) cells. (C) Representative dot plots show the percentages of PD1+CD8+ T cells. (D) Representative dot plots show the percentages of PD1+CD4+ T cells. (E) proportion of CD8+ T cells. (F) Proportion of CD4+ T cells. (G) Changes in CD8+/CD4+ T cells ratio. (H) Proportion of Treg cells. (I) Proportion of PD1+CD8+ T cells. (J) proportion of PD1+CD4+ T cells. (K) Absolute numbers of CD8+ TILs. (L) Absolute numbers of CD4+ TILs. (M) The ratio of CD8+/CD4+ T cells. (N) Absolute numbers of Tregs. (O) Absolute numbers of PD1+CD8+ TILs. (P) Absolute numbers of PD1+CD4+ TILs. One-way analysis of variance and Dunnett's test were used to compare immune cell fraction differences between treated groups and control groups, statistical significance was set at $p<0.05$. *, $p<0.05$; **, $p<0.01$; ****, $p<0.0001$. RT, radiotherapy; TILs tumor infiltrating lymphocytes; Tregs, regulatory T.

J Immunother Cancer: first published as 10.1136/jitc-2020-000826 on 26 October 2020. Downloaded from http://jitc.bmj.com/ on April 28, 2024 by guest. Protected by copyright.

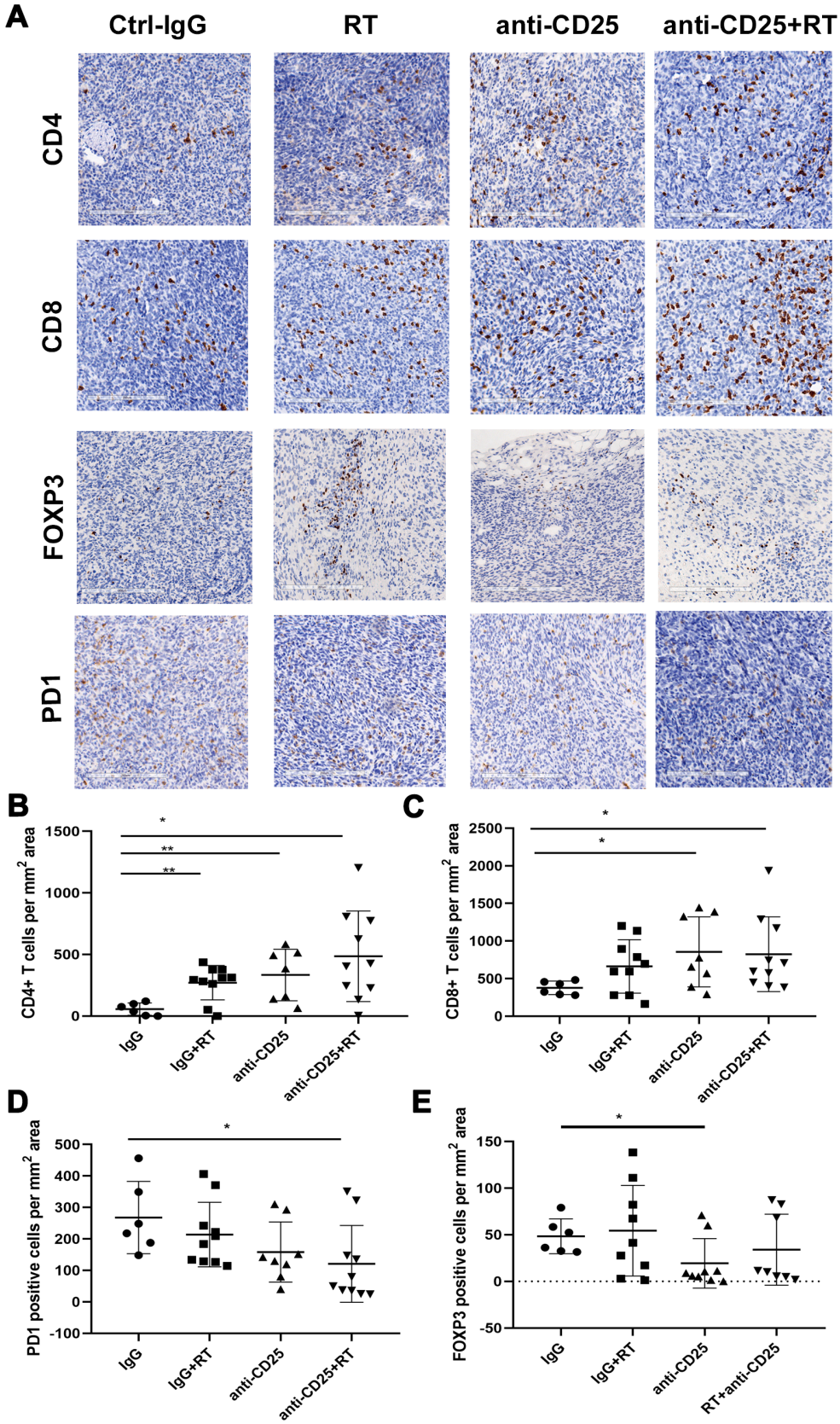

Figure 4 Single-dose RT combined with anti-CD25 changes the expression of CD4, CD8, FOXP3 and PD1 in unirradiated tumors. (A) Expression of CD4, CD8, FOXP3 and PD1 in unirradiated tumors using IHC analysis. The positive staining was expressed as brown. (B–E) The quantifications of CD4+, CD8+, PD1+ and FOXP3+ cells were performed using the software Aperio image scope. One-way analysis of variance and Dunnett's test were used to compare immune cell number differences between treated groups and control groups, statistical significance was set at $p<0.05$, *, $p<0.05$; **, $p<0.01$. IHC, immunohistochemistry; RT, radiotherapy.

J Immunother Cancer: first published as 10.1136/jitc-2020-000826 on 26 October 2020. Downloaded from http://jitc.bmj.com/ on April 28, 2024 by guest. Protected by copyright.

percentage of CD4+ T cells although anti-CD25 decreased the proportion of CD4+ T cells(p=0.0003). Anti-CD25 decreased the proportion of Tregs (CD4+Foxp3+ T cells) (p=0.042). The percentage of CD8+ or CD4+ T cells expressing Granzyme B increased in RT and combination therapy groups compared with those in control group, although the difference was not significant. No significant difference was observed in the percentages of CD4+CD69+or CD8+CD69+ T cells among groups (online supplemental figure 8A–C).

In the unirradiated tumors, both radiotherapy and combination therapy significantly increased the proportion of CD4+ T cells as compared with control (p=0.0008, p=0.025, respectively). Tregs decreased after anti-CD25 treatment as compared with control group (p=0.0148). The percentage of CD4+ T cells expressing Granzyme B increased in combination therapy group compared with that in control group, although there was no significance. No significant difference was observed in the percentages of CD8+CD69+, CD4+PD1+ and CD8+PD1+ T cells among groups (online supplemental figure 8D).

In blood, anti-CD25 and combination therapy significantly decreased the proportion of Tregs relative to the IgG control (p=0.001, p=0.0028, respectively). Radiotherapy and anti-CD25 increased the proportion of CD8+CD69+ T cells compared with control (p=0.0436, p=0.041, respectively). No significant difference was observed in the percentages of CD4+, CD8+ and CD4+CD69+ T cells among groups (online supplemental figure 8E,F).

Rt combined with anti-CTLA4 and anti-PD1 enhances control of irradiated tumors and liver metastasis

To determine the optimal dose of anti-CTLA4, we investigated the effect of the in vivo administration of anti-CTLA4 on the CD25+Foxp3+ population in spleens and tumor tissues. As shown in online supplemental figure 9, CTLA4 did not induce the decrease of Treg cells in spleen. In tumor, CD25+Foxp3+ cells reduced maximally on days 2–4 and fully recovered by day 8 after a single in vivo administration of 0.25 mg anti-CTLA4 mAb. The reduction was observed in the range of 35%–51% at doses between 0.125 and 0.5 mg. For subsequent analyzes, we used a single injection of 0.25 mg anti-CTLA4.

Mice-bearing synchronous CRC liver metastasis were used as a model to investigate the effects of radiotherapy combination with anti-CTLA4 and anti-PD1 mAbs in local and liver metastasis. For single-dose radiotherapy, radiotherapy at dose of 8 Gy was applied only to the right leg tumor site (figure 5A). We found that RT+IgG, RT+anti-CTLA4 and RT+anti-CTLA4+PD1 could control local tumors (p<0.0001). The best response in both tumors occurred with RT+anti-CTLA4+PD1 (figure 5B–E). RT+IgG, RT+anti-CTLA4 and RT+anti-CTLA4+PD1 also resulted in decreased number of liver metastatic nodules as compared with the IgG control with average liver surface metastatic nodules of 2.5±3.3; 1.3±1.9; 0.33±0.5; 8.5±6.8 for RT+IgG, RT+ anti-CTLA4, RT+ anti-CTLA4+PD1 and IgG respectively (p=0.082, p=0.0337 and p=0.0157, respectively) (figure 5B,F,G). The volume of liver metastatic nodules in RT+ anti-CTLA4 group was smaller than RT+ IgG.

We also performed dose-fractionated radiotherapy regimen (5 fractions of 2.3 Gy each) on synchronous CRC liver metastasis model (figure 6A). The results were similar with that of single dose. We found that RT+ anti-CTLA4 and RT+ anti-CTLA4+PD1 could control local tumors (p=0.0053, p=0.0015, respectively) (figure 6B). RT+ IgG, anti-CTLA4, RT+ anti-CTLA4 and RT+ anti-CTLA4+PD1 also resulted in decreased number of liver metastatic nodules as compared with IgG control with average liver surface metastatic nodules of 4.17±2.9; 3.4±2.3; 2.8±1.92; 1.71±3.4; 10±4.06 for RT +IgG, anti-CTLA4, RT+ anti-CTLA4, RT+ anti-CTLA4+PD1 and IgG respectively (p=0.0217, p=0.0134, p=0.0072 and p=0.0032, respectively) (figure 6C).

RT combined with anti-CTLA4 and anti-PD1 changes the immune tumor microenvironment in irradiated and synchronous liver metastatic lesions

In the single-dose radiotherapy model, changes in TIL proportions showed similar trends in irradiated tumor, blood and liver metastases. In liver metastases, combination therapy (RT and anti-CTLA4 or RT and anti-CTLA4+ anti-PD1) induced an increase in the percentage of CD8+ T cells (p=0.06, p=0.002, p=0.2081 for RT vs control, RT+ anti-CTLA4 vs control, RT+ anti-CTLA4+ anti-PD1 vs control, respectively) and the ratio of CD8+/CD4+ (p=0.0219, p=0.0002, p=0.0363 for RT vs control, RT+ anti-CTLA4 vs control, RT+ anti-CTLA4+ anti-PD1 vs control, respectively) relative to the IgG control groups. A decrease in the percentages of CD4+ T cells was observed in RT (p=0.0088) and combination therapy groups (p<0.0001 and p=0.0075 for RT+ anti-CTLA4 and RT+ anti-CTLA4+ anti-PD1, respectively) compared with control. Combination therapy could decrease the proportion of Tregs (p=0.0477, p=0.0178 for RT+ anti-CTLA4 and RT+ anti-CTLA4+ anti-PD1, respectively). Combined therapy increased the expression of CD44 in CD4+ (p=0.026, p=0.0086 for RT+ anti-CTLA4 and RT+ anti-CTLA4+ anti-PD1, respectively) and in CD8+ T cells (p=0.035 for RT+ anti-CTLA4+ anti-PD1) (figure 5H, online supplemental figure 10).

Combined therapy decreased PD-1 expression in CD8+cells (p=0.029, p=0.091 for RT+ anti-CTLA4 and RT+ anti-CTLA4+ anti-PD1, respectively), but increased PD-1 expression in CD4+ cells in liver metastasis without significant difference (p=0.21, p=0.12 for RT+ anti-CTLA4 and RT+ anti-CTLA4+ anti-PD1, respectively) (figure 5H, online supplemental figure 10).

Changes in TILs proportion showed similar trends in irradiated tumor, blood and liver metastases (online supplemental figure 11).

Combined therapy reversed the increase of PD-1 expression in CD4+ and CD8+ T cells in blood (for CD4+PD1+ cells, p=0.0002 for RT+ anti-CTLA4 vs RT, p<0.0001 for RT+ anti-CTLA4+ anti-PD1 vs RT; for CD8 +PD1+cells,

J Immunother Cancer: first published as 10.1136/jitc-2020-000826 on 26 October 2020. Downloaded from http://jitc.bmj.com/ on April 28, 2024 by guest. Protected by copyright.

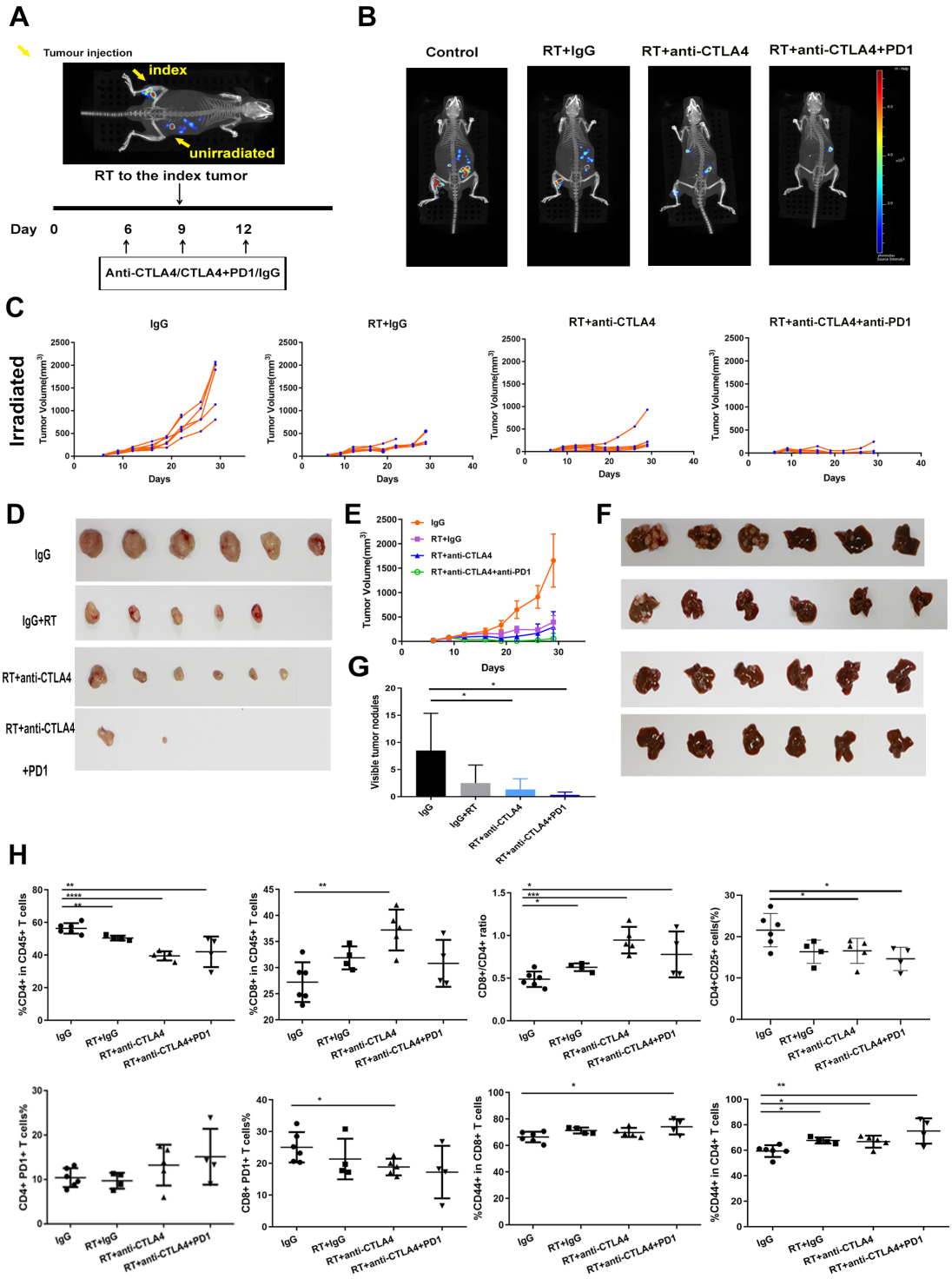

Figure 5 Single-dose RT combined with anti-CTLA4/and anti-PD1 enhances tumor growth control in a synchronous CRC liver metastasis mouse model. (A) Schematic of the experimental setup. Yellow arrow: location of transplantation. Timeline starts from original tumor implantation (day 0). Black arrows: treatments given. (B) IVIS Spectrum-CT images of RT combined with anti-CTLA4/and anti-PD1-treated primary tumors and liver metastases. (C–E) Total irradiated tumor growth for MC38 tumors after the indicated treatment. Control: IgG (n=6); RT: IgG+RT (n=6); RT+ anti–CTLA4 (n=6); RT+ anti-CTLA4+ anti-PD1 (n=6). Using a mixed effect linear model to compare tumor growth differences between treated groups and control groups. (F) Representative livers derived from mice are show. (G) Quantification of liver metastasis. One-way analysis of variance and Student's t test were used to compare liver metastasis number differences between treated groups and control groups. (H) The percentages of CD4+, CD8+ T cells, Tregs, PD1+CD8+/CD4+ and CD44+CD8+/CD4+ T cells after gating on CD45+ cells analyzed by flow cytometry in the liver metastasis-derived cell suspensions corresponding to RT, RT+ anti-CTLA4, RT+ anti-CTLA4+ anti-PD1 as indicated. One-way analysis of variance and Dunnett's test were used to compare immune cell fraction differences between treated groups and control groups, statistical significance was set at $p<0.05$, *, $p<0.05$; **, $p<0.01$; ***, $p<0.001$; ****, $p<0.0001$. CRC, colorectal cancer; RT, radiotherapy; Tregs, regulatory T.

J Immunother Cancer: first published as 10.1136/jitc-2020-000826 on 26 October 2020. Downloaded from http://jitc.bmj.com/ on April 28, 2024 by guest. Protected by copyright.

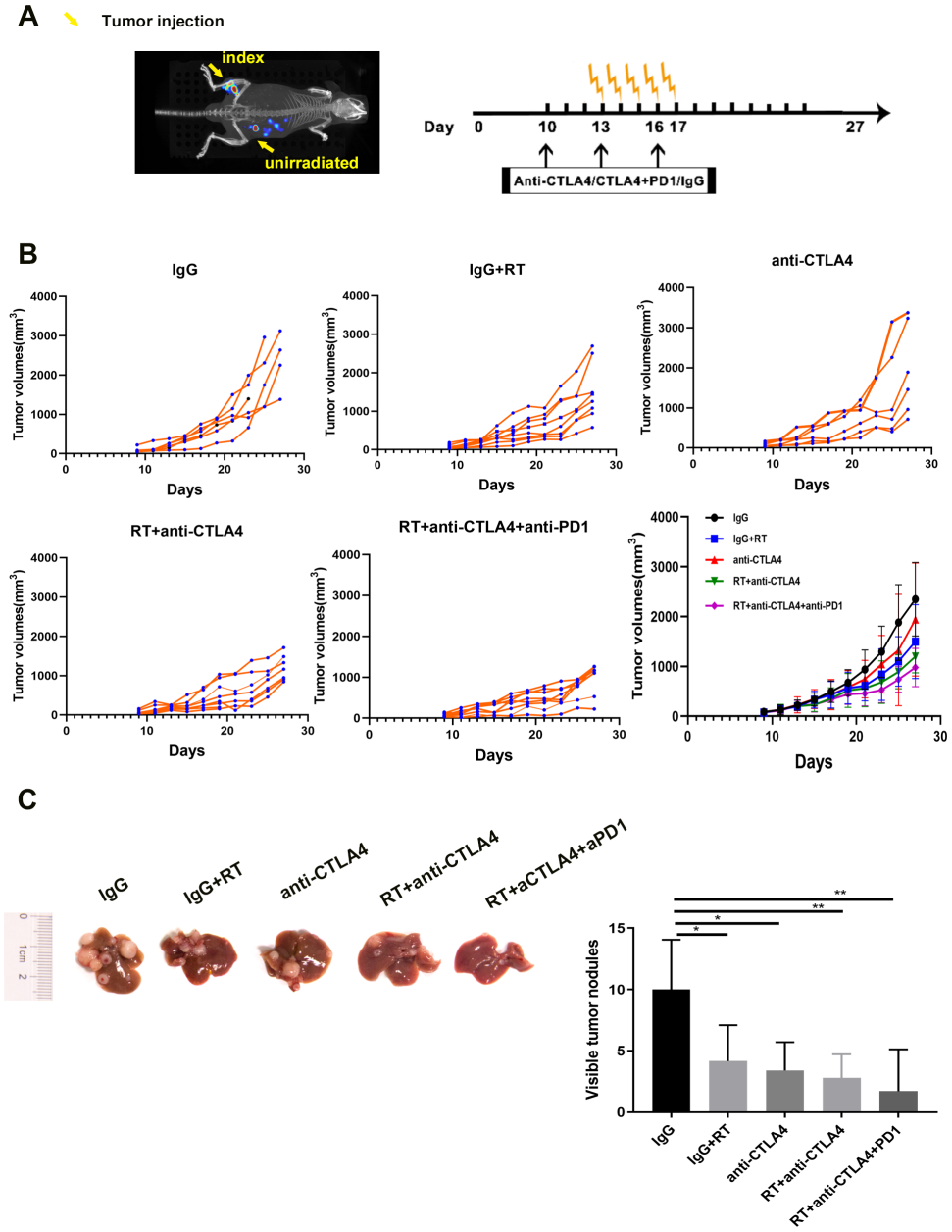

Figure 6 Dose-fractionated RT combined with anti-CTLA4/and anti-PD1 enhances tumor growth control in a synchronous CRC liver metastasis mouse model. (A) Schematic of the experimental setup. Yellow arrow: radiotherapy given (5 fractions of 2.3 Gy each). Timeline starts from original tumor implantation (day 0). Black arrows: drug treatments given. (B) Total irradiated tumor growth for MC38 tumors after the indicated treatment. Control: IgG (n=7); radiotherapy: IgG+RT (n=8); Anti-CTLA4 (n=6); RT+ anti-CTLA4 (n=7); RT+ anti–CTLA4+ anti-PD1 (n=8). Student's t-test was used to compare tumor volume differences between treated groups and control groups. (C) Representative livers derived from mice are shown. (D) Quantification of liver metastasis. Student's t-test was used to compare liver metastasis number differences between treated groups and control groups, statistical significance was set at p<0.05, *, p<0.05; **, p<0.01. CRC, colorectal cancer; RT, radiotherapy.

p=0.0124 for RT+ anti-CTLA4 vs RT, p=0.0003 for RT+ anti-CTLA4+ anti-PD1 vs RT) after radiotherapy (online supplemental figure 11).

RT increased the expression of PD-1 in CD8+ (p=0.078) and CD4+ T (p=0.049) cells in irradiated tumors. However, there was no significant difference between RT and RT+CTLA4 groups (online supplemental figure 11).

For the dose-fractionated radiotherapy model, in the irradiated tumors, combination therapy (RT and anti-CTLA4 or RT and anti-CTLA4+ anti-PD1) induced an increase in CD8+ T cells number (p=0.0488 for RT+ anti-CTLA4 vs control, p=0.0663 for RT+ anti-CTLA4+ anti-PD1 vs control, respectively) and the ratio of CD8+/CD4+ (p=0.0102 for RT+ anti-CTLA4 vs control, p=0.0088 for RT+ anti-CTLA4+ anti-PD1 vs control, respectively) relative to the IgG control. No significant difference was observed in the number of CD4+ T cells and Tregs among groups. We found that combination therapy (RT and anti-CTLA4 or RT and anti-CTLA4+ anti-PD1) significantly increased the number of CD69+CD8+ T cells

J Immunother Cancer: first published as 10.1136/jitc-2020-000826 on 26 October 2020. Downloaded from http://jitc.bmj.com/ on April 28, 2024 by guest. Protected by copyright.

(p=0.044 for RT+ anti-CTLA4 vs control, p=0.0334 for RT+ anti-CTLA4+ anti-PD1 vs control, respectively). RT or RT and anti-CTLA4+ anti-PD1 increased the number of CD69+CD4+ T cells (p=0.0394 for RT vs control, p=0.0472 for RT+ anti-CTLA4+ anti-PD1 vs control, respectively) (figure 7A,B).

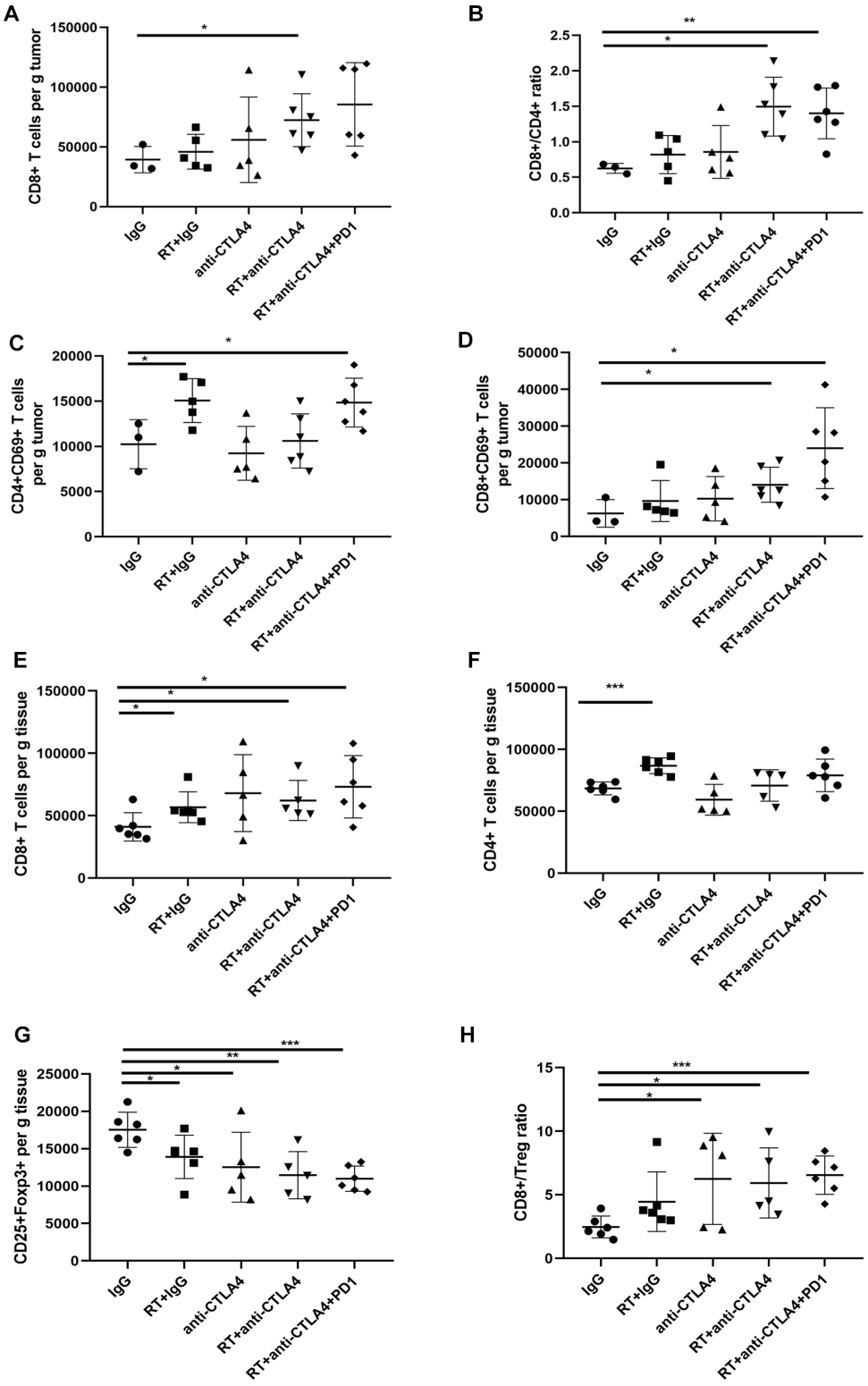

Figure 7 Dose-fractionated RT combined with anti-CTLA4/and anti-PD1 changes the fractions of CD4+, CD8+ and Tregs cells in irradiated tumors and liver metastasis. (A–D) Absolute numbers of CD8+, CD4+CD69+, CD8+CD69+ T cells and ratio of CD8/CD4 T cells in irradiated tumors. (E–H) Absolute numbers of CD8+, CD4+, CD25+Foxp3+ T cells and ratio of CD8/Treg cells in liver. Dunnet t-test was used to compare immune cell fraction differences between treated groups and control groups, statistical significance was set at p<0.05, *, p<0.05; **, p<0.01; ***, p<0.001. RT, radiotherapy; Tregs, regulatory T.

J Immunother Cancer: first published as 10.1136/jitc-2020-000826 on 26 October 2020. Downloaded from http://jitc.bmj.com/ on April 28, 2024 by guest. Protected by copyright.

In liver metastases, RT increased the number of CD8+ Tand CD4+ T cells (p=0.0451and p=0.0003, respectively). Combination therapy (RT and anti-CTLA4 or RT and anti-CTLA4+ anti-PD1) induced an increase in the numbers of CD8+ T cells (p=0.0308 for RT+ anti-CTLA4 vs control, p=0.0168 for RT+ anti-CTLA4+ anti-PD1 vs control, respectively). Combination therapy could significantly decrease the numbers of Tregs (p=0.038 for RT vs control, p=0.0457 for anti-CTLA4, p=0.0052 for RT+ anti-CTLA4 vs control, p=0.0002 for RT+ anti-CTLA4+ anti-PD1 vs control) and increase the ratio of CD8+/Treg (p=0.0326 for anti-CTLA4, p=0.0165 for RT+ anti-CTLA4 vs control, p=0.0002 for RT+ anti-CTLA4+ anti-PD1 vs control, respectively) (figure 7C,D). No significant difference was observed in the percentages of CD4+ T cells, CD8+ T cells and Tregs among groups in blood.

DISCUSSION

We analyzed pretreatment tumor biopsies to identify the genes which were correlated with prognosis of LARC treated with nRT. Our study indicated that the protective genes were enriched in the immune activation-related pathways, mainly composed of cytokine signaling in immune system, signaling by IL, downstream signaling events of B cell receptor, IL-4 and 13 signaling. The presence of a pre-existing immune response indicates a more favorable prognosis than that of patients whose tumors lack these features in rectal cancer pretreated with nCRT.

Many previous studies have shown that intratumoral immune cells infiltrate is the most important predictive criterium for patient survival.[18] We further analyzed correlation between the infiltration of specific immune cell subsets and prognosis. Our results demonstrated that heterogeneous immune cell infiltration was present in patients with good and poor prognosis. The presence of Tregs and resting DCs in pre-nRT biopsies correlated with tumor recurrence and survival. In most tumor types, the tumor microenvironment is dominated by immunosuppression elements. The immunosuppressive tumor microenvironment composed by immune-suppressive cytokines, molecules, and cells inhibits effective antitumor immunity. Treg cells, one of the most common immune-suppressive cells in tumors, suppress antitumor immunity, thereby promoting cancer progression.[19] It was reported that stromal Foxp3+ cell density in post-CRT surgical samples was strongly associated with TRG and was negatively associated with recurrence-free survival.[20] Treg cells impose their suppressive activity via inhibiting the maturation of antigen-presenting cell, consumption of IL-2 via high-affinity receptor CD25 expression, secretion of inhibitory cytokines and killing effector T cells and APCs through expression of granzyme and/or perforin.[21] Resting DCs can present self-antigens to T cells,[22] which leads to immune tolerance either through T cell deletion or the differentiation of regulatory or suppressor T cells.

We also investigated the influence of systemic immune condition on the therapeutic outcome of patients with nCRT. We found that several immunomodulatory cytokines including IL-2,–3, –4 and GM-CSF in pretreatment serum were negatively correlated with the prognosis.

Although high-dose IL-2 could stimulate antitumor cytotoxic lymphocytes, including effector T and NK cells and has shown antitumor immune responses,[23] the low but constant IL-2 production during resting conditions primarily supports the development and homeostatic survival of Treg cells to main peripheral immune tolerance.[24] Low level of IL-2 in pretreatment serum was considered to serve immunosuppressive action by activating Treg cells. IL-2 and Treg cells also have been reported to play negative regulation on DCs. IL-2 inhibits the in vitro development of plasmacytoid DCs and conventional DCs from BM cells cultured with Flt3L.[25] DC numbers are increased in IL-2−/− mice due to an indirect inhibitory effect on IL-2 production and/or Treg cells.[26] Elevated level of GM-CSF in serum has been recognized in patients with CRC and considered a potential diagnostic and prognostic marker associated with poor outcomes.[27] G-CSF has critical roles in MDSCs migration, proliferation and function maintenance.[28] IL-3 was reported to be able to stimulate endothelial cell proliferation, migration and the formation of new blood vessels[29] and could play an important role in tumor vasculogenesis. Higher serum levels of IL-4 were found in metastatic CRC patients.[30] IL-4/IL-4 receptor engagement leads to signal transducer and activator of transcription 6 phosphorylation.[31] In a mouse model of colitis-associated colon cancer, signaling through IL-4 receptor α promoted tumor growth.[32] We further found that serum TNFα level in post-nCRT was positively correlated with prognosis. TNF can promote the activation and proliferation of naïve and effector T cells, but also can induce apoptosis of highly activated effector T cells. Moreover, TNF can downregulate the suppressive capacity of Tregs.[33] TNF-α enhanced tumor control when combined with radiotherapy (RT) in an animal colon cancer model.[34]

Therefore, we hypothesized that the immunosuppressive factors, especially Tregs may play an important role in rectal cancer relapse and hamper the therapeutic outcome of nCRT. Our preclinical mouse experiment results demonstrated that radiotherapy combination with Tregs depletion transiently using anti-CD25 or CTLA4 could enhance the efficiency of radiotherapy and improve the survival.

Recent interest in the abscopal effect from radiotherapy to treatment of both localized and metastatic disease motivated us to investigate the abscopal effect of RT on metastatic rectal cancer. The abscopal effect refers to radiotherapy-induced tumor regression in lesions distant from the irradiated site.[35]

RT may enhance the endogenous T-cell response to primary tumors and their antigens,[13] which improves local and systemic antitumor immunotherapeutic efficacy.[36]

Our retrospective review showed rarity of rectal cancer patients with distant metastasis or synchronous extracolonic cancers obtained nCRT, indicating that there was a

J Immunother Cancer: first published as 10.1136/jitc-2020-000826 on 26 October 2020. Downloaded from http://jitc.bmj.com/ on April 28, 2024 by guest. Protected by copyright.

high threshold on the potency of immune activation to translate into a clinically relevant response. The abscopal response was seen only in some patients with metastases, not seen in patients with synchronous extracolonic cancer. The abscopal effect relies on tumor specified CD8 T cell activity and overcoming the immunosuppressive barrier. When a tumor is irradiated, ionizing radiation may lead to the release of tumor-associated antigens which can stimulate a tumor-specific immune response, with the recruitment and activation of antigen-presenting cells, and CD8+ T cells activation. Once activated, cytotoxic T lymphocytes migrate to the irradiated tumor and eliminate residual cancer cells and also to distant metastatic sites, leading to systemic tumor regression.[37] Absence of the abscopal effect in synchronous extracolonic cancer might be due to that synchronous multiple cancers have independent genetic origins, acquire dissimilar somatic alterations, and have different clone composition.[38] Different responses were observed among different metastasis with distinct tumor-immune microenvironments. The regressing liver metastases were infiltrated by CD8+ T cells, whereas stable and progressing metastases exhibited Tregs and PD1+CD8/PD1+CD4 T cells infiltration. The heterogeneity could be due to the relative weakness of the immunizing effects and concomitantly elicited immunosuppressing factors. Several studies showed that patients with metastatic CRC cells from primary and metastatic sites exhibited heterogeneity at the genomic level.[39] The tumor heterogeneity increases the likelihood of presence of subclones which is able to escape the immune system.[40] In addition, RT may be able to disclose cryptic tumor antigens, tumor cell-induced immune-suppression and immune-tolerance hamper the development of therapeutically effective antitumor immune responses.[41] The Tregs have been shown to persist in the tumor microenvironment at a relative high frequency after radiation, which is thought to result from their intrinsic radiation resistance.[41] Our in vivo animal study demonstrated that single-dose radiotherapy induced not only CD8, CD4 infiltration in irradiated and unirradiated tumors but also Treg cells infiltration and TILs expressing high levels of PD-1. Combination of radiotherapy and anti-CD25 treatment had a better unirradiated tumor growth control and survival, but did not show better effect on local tumor control than RT alone. The combination treatment resulted in increased CD8+ T cells and decreased PD1+CD8+ T cells, PD1+CD4+ T cells and Tregs in local tumors. In unirradiated tumors, anti-CD25 increased the number of CD8 T cells and reduced the rise of Treg cells induced by radiotherapy.

Our retrospective study suggested that the infiltration of PD1+ T cells and Tregs may limit the abscopal response in liver metastasis. The bilateral subcutaneous tumor mouse model is a limited recapitulation of the tumor microenvironments of metastatic tumors in patients. To better understand the effects of radiotherapy in combination with anti-CTLA4 and anti-PD1 mAbs on liver metastasis, a synchronous CRC liver metastasis model was used in this study. Combination treatment could inhibit liver metastasis and enhance abscopal response by inhibiting immunosuppressive Treg cells, reversing T cells exhaustion and further promoting T cell activation.

To mimic the regimen used in routine clinical practice, we performed dose-fractionated radiotherapy regimen in bilateral tumors and synchronous CRC liver metastasis mice models. Some studies have demonstrated the superiority of single or fractional radiotherapy in antitumor immune response. In our study, single doses of 12 Gy and 8 Gy could significantly inhibit the growth of the primary tumor and distant tumor, but a single dose of 12 Gy increased the proportion of Treg cells. Our result is similar to Son *et al*'s results.[42] Schaue et al's study in the B16-OVA murine melanoma model found that single doses of 7.5 and 10 Gy could control tumor growth was associated with a decrease in the proportion of Tregs and an increase in T cell response in the spleen. However, a single dose of 15 Gy increased both effector and Treg cells.[43]

Our study showed that low-dose daily fractionated radiotherapy (5 fractions of 2.3 Gy each) could lead to T-cell activation at the site of treatment and T-cell infiltration at the unirradiated site, but did not induce the increase in Tregs. Dose-fractionated radiotherapy combined with anti-CD25 or anti-CTLA4/and anti-PD1 mAbs could significantly decrease immunosuppressive Treg cells in unirradiated tumor or liver metastasis. A recent study found that low-dose daily fractionated radiotherapy resulted in the infiltration and expansion of polyclonal T cells in the treatment site, but inhibited the systemic antitumor immunity through the PD-1/PD-L1.[44] It was reported that low-dose daily fractionated radiotherapy could induce an immunostimulatory macrophage phenotype.[45] To date, no established consensus on the most immunogenic radiation dose and schedule in the clinical and preclinical setting. Obviously, further study is needed to directly compare the immunogenicity of different radiotherapy dose fractionation schemes.

In our retrospective study, we also analyzed a metachronous liver metastasis from a patient with rectal cancer treated with nCRT to observe the effect of tumor microenvironment on liver metastasis formation after nCRT. Higher Foxp3 positive T cell infiltration was observed and these changes were pronounced in the stromal, which indicated that the immunosuppressive tumor microenvironment in liver might promote the formation of metastasis. Combination of radiotherapy and suppression of Tregs could treat existing metastases as well as prevent future metastases. Our results suggest that the addition of ICB to radiotherapy could potentially generate antitumor immune responses, which could treat existing metastases as well as prevent future metastases. Combination of RT and ICB could be used to prevent recurrences and metastases in early-stage rectal cancer treatment.

Recently, there have been efforts and success in utilizing ICB and other immunotherapeutic strategies in earlier disease stages, including the first-line metastatic setting and adjuvant setting for locally advanced disease.

J Immunother Cancer: first published as 10.1136/jitc-2020-000826 on 26 October 2020. Downloaded from http://jitc.bmj.com/ on April 28, 2024 by guest. Protected by copyright.

It has been shown that durvalumab given after definitive chemoradiation significantly prolonged PFS compared with placebo in stage III non-small cell lung cancer (NSCLC).[46] The results from a phase I pembrolizumab trial, KEYNOTE-001, showed that patients with advanced NSCLC who had previously received radiotherapy had significantly longer PFS and OS than those who received placebo.[47]

There are several limitations in this study. Anti-CD25 does not exclusively deplete Tregs. It was reported that CD25 is constitutively expressed on Treg cells but not on the naive Teff cells. When Teff cells are activated, CD25 will be upregulated transiently.[48] Anti-CD25 could also deplete CD4+ and CD8+ effectors transiently expressing CD25.[49] However, Arce Vargas *et al*[50] reported that CD25 expression is largely restricted to tumor-infiltrating Treg cells in mice and humans. For colorectal carcinoma mice model, the percentage of CD25 expressing CD4+FoxP3+ Treg cells within tumor was significantly higher than CD4+FoxP3 and CD8+ Teff cells. The expression of CD25 on TILs in tumor patients remained largely restricted to CD4+FoxP3+ Treg cells, similar with mice models. In our study, we also found that the percentage of CD25-expressing Teff cells (CD8+=0.4%–1.6%, CD4+FoxP3-=10.3%–19.2%) was significantly lower than on Treg cells (59.2%–68.5%) and anti-CD25 did not affect the effector T cell subsets. Therefore, the effects of the anti-CD25 were predominantly directed against Treg cells.

The patient cohorts in our study received different treatment regimens. The patients in cohort 1 received an intermediate-fraction preoperative radiotherapy regime consisting of 30 Gy delivered in 10 daily fractions. The patients in cohort 2 and 3 received a long-course preoperative radiotherapy regime which consisted of a 50.6 Gy dose delivered in 22 fractions in combination with chemotherapy. There was no significant difference in local recurrence rate, distant metastasis and OS between the long-course and intermediate-course regime. The pathological complete response rate with long-course regime was superior to intermediate-course regimen, which may be related to the prolonged treatment time of nRT, or an increased interval between nRT and surgery.[51] Radiation dose and fraction schedule are related to tumor–host interaction, including local and abscopal antitumor immune response. To date, no clinical studies have directly compared the abscopal effect or immunogenicity among different dose-fractionation regimens. And there is no established consensus on the optimal dose and schedule in the preclinical setting. In future studies, we need to further investigate the effects of different regimes on the tumor microenvironment, especially the long-term regime. It will be interesting to see how to optimally combine radiation and blocking and depleting activity of specific immune modulatory antibodies to achieve the best therapeutic benefits. The suitable time to initiate the immune modulatory antibodies therapy will also need to be determined.

In our study, the cohort 3 is small in size. According to National Comprehensive Cancer Network (NCCN) guideline, for stage IV rectal cancer patients with resectable or potentially resectable metastasis, chemotherapy plus primary tumor radiotherapy or surgical resection is recommended. However, patients with resectable primary rectal tumor and resectable synchronous metastases are limited. A larger cohort is needed to validate our results.

The lack of an anti-CTLA4 treatment group in single dose radiotherapy-synchronous CRC liver metastasis experiment is a limitation, which makes us unable to estimate the role of anti-CLTA4 in tumor control. In the dose-fractionated radiotherapy- synchronous CRC liver metastasis experiment, we added anti-CTLA4 treatment group and found that anti-CTLA4 alone could inhibit tumor growth and liver metastasis.

Another limitation is the lack of anti-PD-1+RT group in the metastatic model. Our previous work demonstrated that RT combined with anti-PD1 enhanced the control of tumor growth in a single dose radiotherapy mice model.[52] Dovedi *et al*'s work showed that the combination of fractionated radiotherapy and anti-PD1 generated systemic antitumor responses and tumor control in both irradiated tumor and abscopal effect.[44] In our future study, we plan to investigate the effect of combination of anti-PD1 and RT on rectal cancer metastasis, and compare the effects of RT combined with CTLA4 and PD1.

CONCLUSION

In this study, our results demonstrated that tumor microenvironment is correlated with prognosis of rectal cancer following nCRT. Tregs are related to the recurrence of tumors after radiation therapy and poor prognosis. The heterogeneous abscopal effect of radiotherapy on different metastatic or synchronous extracolonic cancer might have been due to distinct tumor immune microenvironments within different lesions. Our results indicate that depleting Tregs with anti-CD25 or anti-CTLA4 may enhance the effect of radiation therapy to control both local and systemic tumors and has the potential to significantly improve clinical outcomes.

Author affiliations
[1]Key Laboratory of Carcinogenesis and Translational Research, Department of Gastrointestinal Surgery III, Peking University Cancer Hospital & Institute, Beijing, China
[2]School of Life Sciences, Tsinghua University, Beijing, China
[3]Peking-Tsinghua Center for Life Science, Peking University, Bejing, China
[4]Department of Radiation Oncology, Key laboratory of Carcinogenesis and Translational Research, Peking University Cancer Hospital & Institute, Beijing, China
[5]Department of Obstetrics and Gynecology, The Second Hospital of Hebei Medical University, Shijiazhuang, Hebei, China
[6]Department of Gastrointestinal Surgery, Peking University S.G. Hospital, Beijing, China

Acknowledgements The authors would like to thank Dr. Bin Dong, the Department of Pathology, Peking University Cancer Hospital & Institute for her technical assistance.

Contributors DJ and CS designed and performed the experiments, prepared the figures and draft the manuscript; YL, JX and YW assisted with analysis of the mRNA

J Immunother Cancer: first published as 10.1136/jitc-2020-000826 on 26 October 2020. Downloaded from http://jitc.bmj.com/ on April 28, 2024 by guest. Protected by copyright.

expression profiling and animal experiments. JJ, XC, and SY contributed to the performance of the experiments; JG supervised the work and wrote the manuscript.

Funding This work was supported by the National Natural Science Foundation (81772565, 81372593, 81201965), Beijing Natural Science Foundation (7132052), and the National High Technology Research and Development Program of China (863 Program) (No.2012AA02A506, 2014AA020801).

Competing interests None declared.

Patient consent for publication Not required.

Ethics approval Sample collection and usage was approved by the Ethics Review Committees of Peking University Cancer Hospital & Institute and in accordance with the Declaration of Helsinki. All animal experiments were reviewed and approved by the Ethics Review Committee at the Peking University Cancer Hospital. All animal experiments were performed following protocols approved by the Institutional Animal Care and Use Committee (IACUC) at the Peking University Cancer Hospital.

Provenance and peer review Not commissioned; externally peer reviewed.

Data availability statement Data are available on reasonable request. The datasets used and/or analysed during the current study are available in the GEO dataset, accession number is GSE119409.

Supplemental material This content has been supplied by the author(s). It has not been vetted by BMJ Publishing Group Limited (BMJ) and may not have been peer-reviewed. Any opinions or recommendations discussed are solely those of the author(s) and are not endorsed by BMJ. BMJ disclaims all liability and responsibility arising from any reliance placed on the content. Where the content includes any translated material, BMJ does not warrant the accuracy and reliability of the translations (including but not limited to local regulations, clinical guidelines, terminology, drug names and drug dosages), and is not responsible for any error and/or omissions arising from translation and adaptation or otherwise.

Open access This is an open access article distributed in accordance with the Creative Commons Attribution Non Commercial (CC BY-NC 4.0) license, which permits others to distribute, remix, adapt, build upon this work non-commercially, and license their derivative works on different terms, provided the original work is properly cited, appropriate credit is given, any changes made indicated, and the use is non-commercial. See http://creativecommons.org/licenses/by-nc/4.0/.

ORCID iD

Jin Gu http://orcid.org/0000-0002-9650-1963

REFERENCES

1 Braendengen M, Tveit KM, Berglund A, *et al*. Randomized phase III study comparing preoperative radiotherapy with chemoradiotherapy in nonresectable rectal cancer. *J Clin Oncol* 2008;26:3687–94.
2 van Gijn W, Marijnen CAM, Nagtegaal ID, *et al*. Preoperative radiotherapy combined with total mesorectal excision for resectable rectal cancer: 12-year follow-up of the multicentre, randomised controlled Tme trial. *Lancet Oncol* 2011;12:575–82.
3 Engelen SME, Maas M, Lahaye MJ, *et al*. Modern multidisciplinary treatment of rectal cancer based on staging with magnetic resonance imaging leads to excellent local control, but distant control remains a challenge. *Eur J Cancer* 2013;49:2311–20.
4 Sauer R, Liersch T, Merkel S, *et al*. Preoperative versus postoperative chemoradiotherapy for locally advanced rectal cancer: results of the German CAO/ARO/AIO-94 randomized phase III trial after a median follow-up of 11 years. *J Clin Oncol* 2012;30:1926–33.
5 Weichselbaum RR, Liang H, Deng L, *et al*. Radiotherapy and immunotherapy: a beneficial liaison? *Nat Rev Clin Oncol* 2017;14:365–79.
6 Postow MA, Callahan MK, Barker CA, *et al*. Immunologic correlates of the abscopal effect in a patient with melanoma. *N Engl J Med* 2012;366:925–31.
7 Wersäll PJ, Blomgren H, Pisa P, *et al*. Regression of non-irradiated metastases after extracranial stereotactic radiotherapy in metastatic renal cell carcinoma. *Acta Oncol* 2006;45:493–7.
8 Hu ZI, McArthur HL, Ho AY. The Abscopal effect of radiation therapy: what is it and how can we use it in breast cancer? *Curr Breast Cancer Rep* 2017;9:45–51.
9 Ohba K, Omagari K, Nakamura T, *et al*. Abscopal regression of hepatocellular carcinoma after radiotherapy for bone metastasis. *Gut* 1998;43:575–7.
10 Golden EB, Chhabra A, Chachoua A, *et al*. Local radiotherapy and granulocyte-macrophage colony-stimulating factor to generate abscopal responses in patients with metastatic solid tumours: a proof-of-principle trial. *Lancet Oncol* 2015;16:795–803.
11 Abuodeh Y, Venkat P, Kim S. Systematic review of case reports on the abscopal effect. *Curr Probl Cancer* 2016;40:25–37.
12 Barker HE, Paget JTE, Khan AA, *et al*. The tumour microenvironment after radiotherapy: mechanisms of resistance and recurrence. *Nat Rev Cancer* 2015;15:409–25.
13 Twyman-Saint Victor C, Rech AJ, Maity A, *et al*. Radiation and dual checkpoint blockade activate non-redundant immune mechanisms in cancer. *Nature* 2015;520:373–7.
14 Rech AJ, Dada H, Kotzin JJ, *et al*. Radiotherapy and CD40 activation separately augment immunity to checkpoint blockade in cancer. *Cancer Res* 2018;78:4282–91.
15 Rodriguez-Ruiz ME, Rodriguez I, Garasa S, *et al*. Abscopal effects of radiotherapy are enhanced by combined immunostimulatory mAbs and are dependent on CD8 T cells and Crosspriming. *Cancer Res* 2016;76:5994–6005.
16 Edge SB BD CC. *Ajcc cancer staging manual*. 7th Ed. Chicago: Springer-Verlag, 2010.
17 Camp RL, Dolled-Filhart M, Rimm DL. X-tile: a new bio-informatics tool for biomarker assessment and outcome-based cut-point optimization. *Clin Cancer Res* 2004;10:7252–9.
18 Bindea G, Mlecnik B, Tosolini M, *et al*. Spatiotemporal dynamics of intratumoral immune cells reveal the immune landscape in human cancer. *Immunity* 2013;39:782–95.
19 Shitara K, Nishikawa H. Regulatory T cells: a potential target in cancer immunotherapy. *Ann N Y Acad Sci* 2018;1417:104–15.
20 McCoy MJ, Hemmings C, Miller TJ, *et al*. Low stromal Foxp3+ regulatory T-cell density is associated with complete response to neoadjuvant chemoradiotherapy in rectal cancer. *Br J Cancer* 2015;113:1677–86.
21 Sakaguchi S, Miyara M, Costantino CM, *et al*. Foxp3+ regulatory T cells in the human immune system. *Nat Rev Immunol* 2010;10:490–500.
22 Palucka K, Banchereau J. Cancer immunotherapy via dendritic cells. *Nat Rev Cancer* 2012;12:265–77.
23 Arenas-Ramirez N, Woytschak J, Boyman O. Interleukin-2: biology, design and application. *Trends Immunol* 2015;36:763–77.
24 Yu A, Snowhite I, Vendrame F, *et al*. Selective IL-2 responsiveness of regulatory T cells through multiple intrinsic mechanisms supports the use of low-dose IL-2 therapy in type 1 diabetes. *Diabetes* 2015;64:2172–83.
25 Lau-Kilby AW, Kretz CC, Pechhold S, *et al*. Interleukin-2 inhibits FMS-like tyrosine kinase 3 receptor ligand (flt3L)-dependent development and function of conventional and plasmacytoid dendritic cells. *Proc Natl Acad Sci U S A* 2011;108:2408–13.
26 Bolton HA, Roediger B, Fazekas de St Groth B. The effects of IL-2 and Treg cells on dendritic cell homeostasis are mediated indirectly via activation of conventional T cells. *Eur J Immunol* 2015;45:1141–7.
27 Taghipour Fard Ardekani M, Malekzadeh M, Hosseini SV, *et al*. Evaluation of pre-treatment serum levels of IL-7 and GM-CSF in colorectal cancer patients. *Int J Mol Cell Med* 2014;3:27–34.
28 Li W, Zhang X, Chen Y, *et al*. G-Csf is a key modulator of MDSC and could be a potential therapeutic target in colitis-associated colorectal cancers. *Protein Cell* 2016;7:130–40.
29 Broughton SE, Dhagat U, Hercus TR, *et al*. The GM-CSF/IL-3/IL-5 cytokine receptor family: from ligand recognition to initiation of signaling. *Immunol Rev* 2012;250:277–302.
30 Kantola T, Klintrup K, Väyrynen JP, *et al*. Stage-Dependent alterations of the serum cytokine pattern in colorectal carcinoma. *Br J Cancer* 2012;107:1729–36.
31 Khaled WT, Read EKC, Nicholson SE, *et al*. The IL-4/IL-13/Stat6 signalling pathway promotes luminal mammary epithelial cell development. *Development* 2007;134:2739–50.
32 Koller FL, Hwang DG, Dozier EA, *et al*. Epithelial interleukin-4 receptor expression promotes colon tumor growth. *Carcinogenesis* 2010;31:1010–7.
33 Mehta AK, Gracias DT, Croft M. Tnf activity and T cells. *Cytokine* 2018;101:14–18.
34 Azria D, Larbouret C, Garambois V, *et al*. A bispecific antibody to enhance radiotherapy by tumor necrosis factor-alpha in human CEA-expressing digestive tumors. *Int J Radiat Oncol Biol Phys* 2004;58:580–8.
35 Ngwa W, Irabor OC, Schoenfeld JD, *et al*. Using immunotherapy to boost the abscopal effect. *Nat Rev Cancer* 2018;18:313–22.
36 Demaria S, Kawashima N, Yang AM, *et al*. Immune-Mediated inhibition of metastases after treatment with local radiation and CTLA-4 blockade in a mouse model of breast cancer. *Clin Cancer Res* 2005;11:728–34.

J Immunother Cancer: first published as 10.1136/jitc-2020-000826 on 26 October 2020. Downloaded from http://jitc.bmj.com/ on April 28, 2024 by guest. Protected by copyright.

37 Rodríguez-Ruiz ME, Vanpouille-Box C, Melero I, *et al*. Immunological mechanisms responsible for radiation-induced Abscopal effect. *Trends Immunol* 2018;39:644–55.
38 Martincorena I, Raine KM, Gerstung M, *et al*. Universal patterns of selection in cancer and somatic tissues. *Cell* 2017;171:e21:1029–41.
39 Wei Q, Ye Z, Zhong X, *et al*. Multiregion whole-exome sequencing of matched primary and metastatic tumors revealed genomic heterogeneity and suggested polyclonal seeding in colorectal cancer metastasis. *Ann Oncol* 2017;28:2135–41.
40 Bhang H-eunC, Ruddy DA, Krishnamurthy Radhakrishna V, *et al*. Studying clonal dynamics in response to cancer therapy using high-complexity barcoding. *Nat Med* 2015;21:440–8.
41 Schaue D, Xie MW, Ratikan JA, *et al*. Regulatory T cells in radiotherapeutic responses. *Front Oncol* 2012;2:90.
42 Son C-H, Bae J-H, Shin D-Y, *et al*. Combination effect of regulatory T-cell depletion and ionizing radiation in mouse models of lung and colon cancer. *Int J Radiat Oncol Biol Phys* 2015;92:390–8.
43 Schaue D, Ratikan JA, Iwamoto KS, *et al*. Maximizing tumor immunity with fractionated radiation. *Int J Radiat Oncol Biol Phys* 2012;83:1306–10.
44 Dovedi SJ, Cheadle EJ, Popple AL, *et al*. Fractionated radiation therapy stimulates antitumor immunity mediated by both resident and infiltrating polyclonal T-cell populations when combined with PD-1 blockade. *Clin Cancer Res* 2017;23:5514–26.
45 Dovedi SJ, Adlard AL, Lipowska-Bhalla G, *et al*. Acquired resistance to fractionated radiotherapy can be overcome by concurrent PD-L1 blockade. *Cancer Res* 2014;74:5458–68.
46 Antonia SJ, Villegas A, Daniel D, *et al*. Durvalumab after chemoradiotherapy in stage III non-small-cell lung cancer. *N Engl J Med* 2017;377:1919–29.
47 Shaverdian N, Lisberg AE, Bornazyan K, *et al*. Previous radiotherapy and the clinical activity and toxicity of pembrolizumab in the treatment of non-small-cell lung cancer: a secondary analysis of the KEYNOTE-001 phase 1 trial. *Lancet Oncol* 2017;18:895–903.
48 Boyman O, Sprent J. The role of interleukin-2 during homeostasis and activation of the immune system. *Nat Rev Immunol* 2012;12:180–90.
49 Ko K, Yamazaki S, Nakamura K, *et al*. Treatment of advanced tumors with agonistic anti-GITR mAb and its effects on tumor-infiltrating Foxp3+CD25+CD4+ regulatory T cells. *J Exp Med* 2005;202:885–91.
50 Arce Vargas F, Furness AJS, Solomon I, *et al*. Fc-Optimized Anti-CD25 depletes tumor-infiltrating regulatory T cells and synergizes with PD-1 blockade to eradicate established tumors. *Immunity* 2017;46:577–86.
51 Zhan T, Gu J, Li M, *et al*. Intermediate-fraction neoadjuvant radiotherapy for rectal cancer. *Dis Colon Rectum* 2013;56:422–32.
52 Ji D, Yi H, Zhang D, *et al*. Somatic mutations and immune alternation in rectal cancer following neoadjuvant chemoradiotherapy. *Cancer Immunol Res* 2018;6:1401–16.

J Immunother Cancer: first published as 10.1136/jitc-2020-000826 on 26 October 2020. Downloaded from http://jitc.bmj.com/ on April 28, 2024 by guest. Protected by copyright.